Weather and Climate Extremes 47 (2025) 100745

Contents lists available at ScienceDirect

Weather and Climate Extremes

journal homepage: www.elsevier.com/locate/wace

# Human-induced climate change increased 2021–2022 drought severity in horn of Africa

Joyce Kimutai [a,b,*], Clair Barnes [a], Mariam Zachariah [a], Sjoukje Y. Philip [c], Sarah F. Kew [c], Izidine Pinto [c], Piotr Wolski [d], Gerbrand Koren [e], Gabriel Vecchi [f,g], Wenchang Yang [f], Sihan Li [h], Maja Vahlberg [i], Roop Singh [i], Dorothy Heinrich [i], Julie Arrighi [i,j,k], Carolina Pereira Marghidan [i,k], Lisa Thalheimer [l,m], Cheikh Kane [i,n], Emmanuel Raju [o,p], Friederike E.L. Otto [a]

[a] Grantham Institute, Imperial College, London, UK
[b] Kenya Meteorological Department, Nairobi, Kenya
[c] Royal Netherlands Meteorological Institute (KNMI), De Bilt, the Netherlands
[d] Climate System Analysis Group, University of Cape Town, Cape Town, South Africa
[e] Copernicus Institute of Sustainable Development, Utrecht University, Utrecht, the Netherlands
[f] Department of Geosciences, Princeton University, Princeton, NJ, 08544, USA
[g] High Meadows, Environmental Institute, Princeton University, Princeton, NJ, 08544, USA
[h] Department of Geography, University of Sheffield, UK
[i] Red Cross Red Crescent Climate Centre, The Hague, the Netherlands
[j] Global Disaster Preparedness Center, Washington DC, USA
[k] Faculty of Geo-Information Science and Earth Observation (ITC), University of Twente, Enschede, the Netherlands
[l] United Nations University, Institute for Environment and Human Security, Bonn, Germany
[m] Princeton School of Public and International Affairs, Princeton University, Princeton, NJ, 08544, USA
[n] Institut de Recherche pour le Développement, U01000/99AA01, Marseille, France
[o] Department of Public Health, Global Health Section & Copenhagen Centre for Disaster Research, University of Copenhagen, Denmark
[p] African Centre for Disaster Studies, North-West University, South Africa

ARTICLE INFO

*Keywords:*
Climate change
Attribution
Drought
Horn of Africa

ABSTRACT

From October 2020 to early 2023, Eastern Africa experienced five consecutive failed (SPEI -2.6) rainy seasons, resulting in the worst drought in 40 years. This led to harvest failures, livestock losses, water scarcity, and conflicts, leaving approximately 4.35 million people in need of humanitarian aid. To understand the role of human-induced climate change in the drought, we analysed rainfall trends and the combined effect of rainfall deficit with high temperatures in the Southern Horn of Africa covering parts of southern Ethiopia, southern Somalia, and eastern Kenya. We employed various climate models and observations to assess changes in 24-month rainfall (2021–2022), and seasonal rainfall; both the (March-April-May, MAM) 'long rains' and (October-November-December, OND) 'short rains' in 2022. We also contextualised the event in terms of vulnerability and exposure to understand how these elements influenced the magnitude of the impacts. Our analysis shows that anthropogenic influence on the combined effects of low rainfall and high evapotranspiration caused by higher temperatures made the drought exceptional, leading to major crop and pasture losses and water shortages. Our results also show a decline in rainfall during MAM and an upward trend during OND, which is attributable to climate change. Despite the wetting trend in OND season, the drought years concluded with successive La Niña conditions, typically linked with below-average rainfall in the region during that season. We do not find a trend in the 24-month precipitation. The assessment on vulnerability and exposure highlights the need for enhanced preparedness of government drought management systems and international aid infrastructure for future severe and prolonged droughts. The study's findings, combined with climate projections that indicate increased heavy precipitation in the region, underscore the pressing necessity for robust adaptation

* Corresponding author. Grantham Institute, Imperial College, London, UK
*E-mail address:* kimutaijoy@gmail.com (J. Kimutai).

https://doi.org/10.1016/j.wace.2025.100745
Received 2 November 2023; Received in revised form 1 September 2024; Accepted 28 January 2025
Available online 6 February 2025
2212-0947/© 2025 The Authors. Published by Elsevier B.V. This is an open access article under the CC BY license (http://creativecommons.org/licenses/by/4.0/).

strategies that can address both wet and dry extremes. The impacts of climate change in Eastern Africa necessitate investments in adaptive measures and resilience building that can evolve with emerging climate signals.

## 1. Introduction

The catastrophic impacts of the recurrent droughts in East Africa continue to worsen. Extended dry conditions punctuated by short intense rainfall events have become commonplace in the region (OCHA, 2023a; Kimutai et al., 2022). The shifts in extreme weather events have substantially increased vulnerability and lowered the adaptive capacity of both human and environmental systems in the region. Eastern Africa experiences two distinct rainy seasons, known as the long rains (occurring from March to May; hereafter MAM) and the short rains (from October to December; hereafter OND), which have significant effects on both the environment and society. In particular, East Africa has experienced an increased frequency of droughts in the MAM season over the past few decades Nicholson (2017); Hoell and Funk (2014) and Funk et al. (2018) linked the drying trend in the period 1981–2016 to intensification of the Indian Ocean branch of the Walker Circulation associated with anomalous warming of north-western Pacific attributable to human influence (Liebmann et al., 2014). related the MAM 1979–2012 drying trend to increased subsidence over the descending branch of the Indian Ocean Walker cell induced by strong upper-level easterlies as a result of human-induced high zonal SST gradient between Indonesia and the central Pacific. Lott et al. (2013) found a role of human influence on enhanced probability of rainfall deficit in MAM 2011. Marthews et al. (2015) and Uhe et al. (2018) however, found no anthropogenic influence on the drought events of MAM 2014; OND 2016 respectively, but could not rule out an influence on surface air temperature and net incoming radiation. Kew et al. (2021) pointed out that determining whether climate change exacerbates droughts in the region depends on which methods are used to calculate water demand as a function of moisture availability and evaporative demand.

The below-average rainfall in the OND 2022 season made it the fifth consecutive failed season since OND 2020. The drought in the 5 consecutive seasons was the worst in 40 years (FAO, 2022; WMO, n.d.). La Niña is known to exert substantial influence on OND rainfall in East Africa and has been associated with most recent intense drought events (e.g., 2010–2011; Lott et al., 2013, 2016; Uhe et al., 2018). Furthermore, co-occurrence of La Niña with a negative phase of the Indian Ocean Dipole (IOD) has been found to exacerbate drought conditions (Schubert et al., 2016). The IOD phase was negative in the most part of 2021 and 2022 (BOM, 2022). Across the region, drought and high food prices weakened many people's ability to grow crops, raise livestock and buy food. The persistent drought conditions led to substantial harvest failure and poor pasture conditions mainly due to decreased surface water availability (WFP, 2022a). Over the period, there was an increased risk of disease, malnutrition, and hunger, which fuelled resource-based conflict and migration (MPI, 2023). Food insecurity and conflict over scarce resources pushed people to migrate to other places within the region (UNHCR, 2023c). At least 180,000 refugees from Somalia and South Sudan crossed into the drought-stricken areas of Kenya and Ethiopia (UNHCR, 2023a).

In Kenya, the government declared a drought emergency in September 2021 (WFP, 2022b.). The drought situation remained critical (alert and alarm drought phases) in 20 of the 23 Arid and Semi-Arid counties until December 2022, when the number of people in need of humanitarian assistance stood at 4.35 million (NDMA, 2022a). Cases of acute malnutrition were reported among 942,000 children aged 6–59 months and 134,000 pregnant or lactating women (UNFPA, 2022). The number of livestock deaths rose to over 2.4 million. These animals are an essential source of livelihood for pastoral communities. By January 2023, close to 9210 metric tonnes of food commodities had been distributed and USD 7.29 million cash-based transfers made (OCHA, 2023d). In early 2023, the government appropriated a further Ksh. 4 billion (approx. USD 30 million) to the nation's drought alleviation programme (Kenya Govt, 2023). Irrespective of the reported rains in most parts of the country by the last Dekad of March (KMD, 2023), the drought conditions did not recover quickly enough to see improvements in food security by mid-2023. In Ethiopia and Somalia, more than 1.7 million people migrated (UNHCR, 2023a) with at least 60,000 school dropouts reported in Ethiopia. By December 2022, up to 7.1 million people in Somalia were at risk of acute malnutrition and in need of urgent humanitarian aid (OCHA, 2023c). More than 1 million people had moved from their homes, a situation that was exacerbated by concurrent conflicts and disease outbreaks.

In this study, we investigate the role of climate change in influencing the intensity and frequency of the 2021–2022 drought in East Africa. Given that previous studies of rainfall deficits have not been conclusive in this region, with some alluding to the influence of other physical factors on drought, we study the hazard using both the basic precipitation deficit and the Standardised Precipitation-Evapotranspiration Index (SPEI). SPEI accounts for the influence of temperature on drought through evapotranspiration in relation to precipitation — a simple water balance. Moreover, we explore the vulnerability and exposure context surrounding the findings of the hazard analysis. In doing so, we highlight possible causes behind the observed impacts, which in turn can inform strategies to prevent or mitigate future impacts, in light of the ongoing climate change. The paper is structured into two parts. Part **I** (section 1- 3) focuses on analysing the hazard (drought) while part **II** (section 4) contextualises the event in terms of vulnerability and exposure.

## 2. Data and methods

### 2.1. Observational data

We utilise three observational datasets; Global Unified Daily Gridded data (CPC; Chen et al., 2008), Climate Hazards Group InfraRed Precipitation with Station data (CHIRPS; Funk et al., 2015b and Centennial Trends (CenTrends; Funk et al., 2015a,b) CPC is a gridded product from NOAA PSL available at $0.5^\circ \times 0.5^\circ$ resolution for the period 1979-present. This source has both rainfall and mean temperature; therefore, we use this as the primary dataset for this study. CHIRPS and CenTrends are state-of-the-art gridded datasets developed by the UC Santa Barbara Climate Hazards Group. CHIRPS is available on a daily timescale for the period 1981–present while CenTrends is a monthly dataset covering 1900–2014. CenTrends and CHIRPS are based on a similar assimilation technique and underlying observational data. The two datasets are highly correlated, with correlations of over 0.95 in the study region during the overlapping period (1981–2014). We therefore extend the CenTrends dataset from 1900 to 2014 with monthly averaged data from CHIRPS from 2015 onward; this dataset is henceforth referred to as the CenTrends-CHIRPS dataset. Time series of precipitation from five stations within the study region were used to evaluate the gridded data products — by comparing the station data with the equivalent time series from the closest cell in the gridded dataset. The three datasets were found to reliably replicate the station time series. Refer to Supplementary Material Figs. S1 and S2 for maps of the locations of the selected stations and comparison plots, respectively.

### 2.2. Event definition

Given that the meteorological drivers of the long and short rains differ, it is useful to distinguish between the climate change signals in the two rainfall seasons for 2021 & 2022 in addition to those in the multi-year drought. This will help to understand the contributions of the individual rainfall seasons to the multi-year drought. Consequently, we choose four temporal definitions: (i) 24-month precipitation (ii) Seasonal average rainfall in MAM; (iii) Seasonal average rainfall in OND rains; and (iv) 2-year Standardised Precipitation Evapotranspiration Index (SPEI). We defined a study domain (Fig. 1; hereafter, EA- 6°S-15°N, 32.5°E-52.5°E) which encompasses the region over which high agro-pastoral impacts (crop harvest losses and drying pasturelands) were reported (Paul, 2022). EA is also fairly homogeneous, both in terms of elevation and climate (see Supplementary Material Fig. S3) but with distinct long and short rain seasons (see Supplementary Material Fig. S4). The region is characterised by arid and semi-arid climates. We obtain SPEI (potential climatic water balance) using rainfall and Potential Evapotranspiration (PET) estimates. Changes in PET i.e., the evaporative demand by the atmosphere, due to regional warming are known to exacerbate droughts in different global regions (e.g., (Arias et al., 2023; Schumacher et al., 2022). It is also expected to increase in the future (Dai, 2013; Greve et al., 2019) as increased radiative forcing from anthropogenic Greenhouse Gas (GHG) increases surface net radiation by inhibiting longwave cooling and increasing vapour pressure deficit as the atmosphere warms (Scheff and Frierson, 2014; Wang et al., 2020). In water-stressed regions, PET is often greater than actual evapotranspiration as the latter is limited by lack of moisture in the soils. Therefore, for areas where latent heat fluxes are or will become limited by moisture supply, PET is expected to increase more than actual evapotranspiration (Jung et al., 2010).

The choice of the PET estimation method in calculating any drought index is subjective but is also limited by the availability of meteorological data and the climatic conditions of the region (Tabari and Aghajanloo, 2012; Trajkovic et al., 2020; Zhao and Ma, 2021). Several studies (Beguería et al., 2014; Dai, 2011; Sheffield et al., 2012; Van Der Schrier et al., 2011) have compared and evaluated the effect of using different PET equations in the calculation of drought indices. While most of these studies recommend methods that factor radiative and aerodynamic processes (e.g, FAO Penman–Monteith; Allen et al., 1998) to those that consider temperature as the main input (e.g., Thornthwaite; Thornthwaite, 1948, Hargreaves-Samani; Hargreaves and Samani, 1985; Baier-Robertson; Baier and Robertson, 1965) those methods commonly require several climatic parameters that are often unavailable in developing countries, especially in remote arid and semi-arid regions. Sheffield et al. (2012) argues that application of radiation-based methods in data-sparse regions often result in unreliable estimates due to uncertainties and errors in the input data or the calibration period (e.g., Van der Schrier et al., 2011; Dai, 2011). A notable limitation is that radiation-based methods tend to overestimate PET in humid regions while temperature-based methods underestimate PET in drylands (e.g, Amatya et al., 1995; Droogers and Allen, 2002; Jensen et al., 1990; Xu and Singh, 2002). For SPEI calculation in this analysis, we do not consider radiation-based methods due to data constraints.

Notwithstanding, we evaluated the sensitivity of SPEI to three temperature-based (Hargreaves-Samani, Baier-Robertson and Thornthwaite) and one radiation-based (Penman–Monteith) PET methods using two distinct datasets. Due to the absence of temperature data in CenTrends-CHIRPS, ERA5 (ECMWF[1] Reanalysis 5th Generation) data is used in the sensitivity analysis. ERA5 dataset is available on the grid size of 0.75 × 0.75 from the 1979 onwards (Hersbach et al., 2020). For the Penman–Monteith method, we utilized pre-calculated ERA5 PET, while for the other methods, PET was derived using maximum and minimum temperature data. As expected, we found relatively higher SPEI trends in Thornthwaite-based estimates compared to Hargreaves, Baier-Robertson and Penman–Monteith (see Supplementary Material Fig. S5) since the Thornthwaite method uses only temperature data which tends to overestimate PET with increasing temperatures (Venkataraman et al., 2016). Although ERA5 PET is calculated using the Penman–Monteith method, which accounts for radiative and aerodynamic processes, we still found similar SPEI trends when compared to the temperature-based estimates. Notwithstanding, Thornthwaite is known to underestimate PET in arid and semiarid regions (Xu and Singh, 2002). The difference in trends is higher for CPC than ERA5. Notably, the Hargreaves-Samani and Baier-Robertson estimations incorporate extra-terrestrial radiation data which has been found to be unreliable in areas with complex terrain or varying meteorological conditions (Feng et al., 2018; G. Li et al., 2017; S. Li et al., 2016; Lujano et al., 2023; Zhang et al., 2020). For instance, they tend to overestimate PET under high relative humidity and underestimate at high wind speed conditions (Almorox et al., 2015; Xu and Singh, 2002; Zhao and Ma, 2021). And like the radiation-based approaches, they have been shown to overestimate PET in humid regions, for example in south-eastern US (Lu et al., 2005) and Serbia (Trajkovic, 2007).

Consequently, in this analysis, we opt to use the Thornthwaite-based PET based on the CPC dataset (see section 2.2 for a detailed description) for the computation of the SPEI index and its associated trends. By utilising the Thornthwaite method, the study makes a careful and contextually relevant selection that accounts for the unique climatic conditions and data constraints of the study region. The consistency in SPEI trends further justifies our choice. We also confirm that the mean downwelling surface radiation over 2021–2022 was sufficient to evaporate the amount of water used as input in the PET estimation (not shown). The implications of this methodological choice on results are discussed in the results section. Fig. 1 shows the drought classification maps for the EA region based on the 24-month (Jan 2021–Dec 2022), and the 3-month (MAM and OND, 2022) SPEI. SPEI is standardised with respect to 1980–2010 climatology. The colour scheme reflects the US Drought Monitor drought classifications (D0 - abnormally dry, D1 - moderate, D2 - severe, D3 - extreme, and D4 - exceptional). Evidently, the two-year drought event was exceptional across a significant portion of the study region, with conditions ranging from moderate to exceptional during the two seasons (SPEI -2.6).

### 2.3. Model and experiment descriptions

We use four multi-model ensembles from climate modelling experiments using very different framings (Philip et al., 2020): Sea Surface temperature (SST) driven global circulation high resolution models, coupled global circulation models and regional climate models. The model descriptions are provided as follows.

- Coordinated Regional Climate Downscaling Experiment (CORDEX)-Africa (0.44° resolution, AFR-44) multi-model ensemble (Nikulin et al., 2012, 2018) comprising of 29 simulations resulting from combinations of 12 Global Climate Models (GCMs) and 8 Regional Climate Models (RCMs). These simulations are composed of historical simulations up to 2005 and extended to the year 2 100 using the RCP8.5 scenario.
- Coordinated Regional Climate Downscaling Experiment (CORDEX)-Africa (0.22° resolution, AFR-22) multi-model ensemble (Gutowski et al., 2016; Giorgi et al., 2021) comprising 10 simulations resulting from combinations of 5 GCMs and 4 RCMs. These simulations are composed of historical simulations up to 2005 and extended to the year 2 100 using the RCP8.5 scenario.
- The FLOR (Vecchi et al., 2014) and AM2.5C360 (Chan et al., 2021; Yang et al., 2021) climate models are developed at Geophysical Fluid Dynamics Laboratory (GFDL). The FLOR model is an atmosphere-ocean coupled GCM with a resolution of 50 km for land

[1] European Centre for Medium-Range Weather Forecasts.

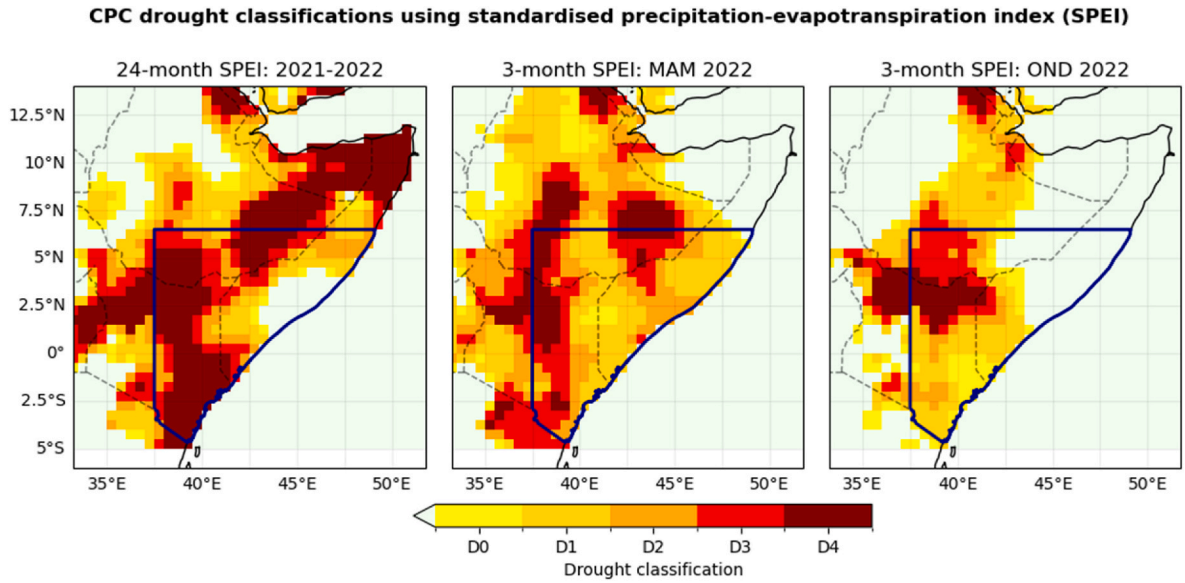


**Fig. 1.** Drought classifications based on Standardised Precipitation Evapotranspiration Index (SPEI), reflecting the drought severity from Jan 2021–Dec 2022 (left), from March–May 2022 (middle), and from Oct–December 2022 (right) relative to the 1980–2010 climatology in the CPC dataset. The bold black outline highlights the study region (EA). Drought classifications: D0 - abnormally dry, D1 - moderate, D2 - severe, D3 - extreme, and D4 – exceptional.

and atmosphere and 1° for ocean and ice. Ten ensemble simulations from FLOR are utilized, which cover the period 1860 to 2 100 and include both the historical and RCP4.5 experiments driven by transient radiative forcings from CMIP5 (Taylor et al., 2012). The AM2.5C360 is an atmospheric GCM based on that in the FLOR model (Delworth et al., 2012; Vecchi et al., 2014) with a horizontal resolution of 25 km. Three ensemble simulations of the Atmospheric Model Intercomparison Project (AMIP) experiment (1871–2050) are analysed. These simulations are initialised from three different pre-industrial conditions but forced by the same SSTs from HadISST1 (Rayner et al., 2003) after groupwise adjustments (Chan et al., 2021) over 1871–2020. SSTs between 2021 and 2050 are using the FLOR RCP4.5 experiment 10-ensemble mean values after bias correction. Radiative forcings are using historical values over 1871–2014 and RCP4.5 values after that.

- HighResMIP SST-forced model ensemble (Haarsma et al., 2016) 11 simulations of which span from 1950 to 2050. The SST and sea ice forcings for the period 1950–2014 are obtained from the 0.25° × 0.25° Hadley Centre Global Sea Ice and Sea Surface Temperature dataset that have undergone area-weighted regridding to match the climate model resolution.

### 2.4. Model evaluation

We evaluated the climate models against the observations in their ability to capture the seasonal cycles, spatial patterns, and the parameters of the fitted models. For the seasonal cycle, we qualitatively compare the model outputs against observations-based plots. We discard the models that fail to capture the bimodal seasonal cycle and/or exhibit ill-defined peaks in their seasonal cycles. We also discard the model if the rainy season onset/cessation varies significantly from the observations. For spatial patterns, models that do not match the observations in terms of the large-scale precipitation patterns are excluded. For model parameters, we exclude any model whose parameter ranges do not overlap with those derived from observations. For distributions that scale with GMST (such as the precipitation-based indices in this study) we evaluate the dispersion parameter, while for those that shift with GMST (in this case, SPEI) we assess the variance parameter (Philip et al., 2020). Based on their performance across these three criteria, models are categorised as 'good,' 'reasonable,' or 'bad.' Per framing or model setup, we also use models that only just pass the evaluation tests if we only have five models or less for that framing that perform well. Due to limitations in observed evapotranspiration products (discussed in Section 2.2), we do not evaluate the models for effective precipitation. Instead, for the SPEI attribution analysis we choose those models that pass the evaluation for both precipitation and temperature. We present model evaluation results in the Supplementary Material Tables S1–S5.

### 2.5. Statistical methods

The attribution analysis steps include: (i) trend calculation from observations; (ii) model evaluation; (iii) multi-method multi-model attribution and (iv) synthesis of the attribution statement. All analyses follow World Weather Attribution (WWA) Protocol, described in Philip et al. (2020), with supporting details found in (van Oldenborgh et al., 2021; Ciavarella et al., 2021). As a measure of anthropogenic climate change, we use the low-pass filtered 4-year smoothed global mean surface temperature (GMST), where GMST is taken from the National Aeronautics and Space Administration (NASA) Goddard Institute for Space Science (GISS) surface temperature analysis (GISTEMP; (Hansen et al., 2010; Lenssen et al., 2019). We calculate the return periods, Probability Ratio (PR; the factor-change in the event's probability) and change in intensity (ΔI) of the event under study to compare the climate of now and of the past. These are defined by the GMST values of now and of the preindustrial period (1850–1900; based on the (globalwarmingindex. To statistically model the event under study, we use Gaussian distributions fitted to the base-10 logarithm of precipitation – hereafter, log10(precip) – and to the 24-month cumulative PET. For precipitation, the distribution is scaled with GMST (and, for OND precipitation, with the detrended Niño3.4 index, as described in Section 2.5.2), while for PET the distribution is shifted with GMST.

#### 2.5.1. Attribution analysis of 24-month rainfall and SPEI

As increased PET associated with regional warming is known to amplify drought impacts (Haile et al., 2020; Nguvava et al., 2019), especially in agriculture, through changes in soil moisture and evapotranspiration rates; we compute the trends and climate change signals in the 24-month SPEI in addition to the 24-month rainfall. We supplement the standard univariate analysis (WWA standard protocol) of the 24-month precipitation by considering joint changes in the 24-month

precipitation and PET using copulas, following Zachariah et al., 2023; Zscheischler and Lehner, 2022. The steps are outlined as follows.

(i) We fit Gaussian distributions that scale and shift with GMST to the base-10 logarithm of observed 24-month precipitation ($X$) and the PET ($Y$) time series, respectively:

$$X \sim Normal(\mu_X, \sigma_X, \alpha_X) \text{ and } Y \sim Normal(\mu_Y, \sigma_Y, \alpha_Y).$$

(ii) We use the cumulative distribution functions (CDFs) of these two distributions to compute the probabilities $u$ and $v$ of exceeding the values observed at each time $t$, so that:

$$u_t = P(X \leq x_t) \text{ and } v_t = 1 - P(Y \leq y_t).$$

Note that since we are interested in the lower tails of the precipitation distribution and the upper tails of the PET distribution, the exceedance probabilities are given by the CDF of $X$ and 1 - the CDF of $Y$.

(iii) The joint cumulative distribution function $C$ is estimated from the marginal exceedance probabilities $u$ and $v$ by fitting a stationary Student's-t copula such that:

$$C(\{u\}, \{v\}) = P(\{U \leq u\}, \{V \leq v\}) \text{ for all } (u, v) \text{ pairs (Nelsen, 2006).}$$

(iv) Contours can be plotted over the subset $\{u, v\} \subset \{U, V\}$ and therefore over the subset $\{x, y\} \subset \{X, Y\}$ that share the same joint exceedance probability $p$, where $1/p$ is the return period of the event.

(v) The univariate distributions fitted in step (i) are used to transform the (u,v) pairs to their equivalent return levels in the current climate and in a 1.2 °C cooler climate (pre-industrial climate) in order to obtain joint return period contours for the current and pre-industrial climates.

#### 2.5.2. Attribution analysis of rainfall

To account for potentially conflicting trends in the MAM and OND rainfall due to regional warming and teleconnection patterns, we supplement the standard WWA approach with additional analyses in an effort to isolate the climate change signal from other confounding effects. OND rainfall in eastern Africa is influenced by phases of the El Niño - Southern Oscillation (ENSO) (Amissah-Arthur et al., 2002; Lott et al., 2013; Mutai and Ward., 2000.; L. A. Ogallo, 1993; L. J. Ogallo, 1988). As a measure of the ENSO, we use the relative Niño3.4 index obtained by subtracting the Niño3.4 index (average SST over 5°S–5°N, 120°–170° W) with the SSTs between 20°S and 20°N to adjust the index for climate change (Van Oldenborgh et al., 2021). Since we are averaging the index over a period of several months, the values are not standardised per calendar month as in that paper. To disentangle the effects of ENSO and GMST, the standard approach is amended to include both relative Nino 3.4 (detrended using tropical SSTs and averaged over OND) and GMST as covariates when fitting the distribution. Using CPC and CenTrends-CHIRPS datasets, we therefore fit two linear regression models; (i) log10(precip) which depends only on GMST and (ii) log10 (precip) which depends on both GMST and relative Niño3.4. So that

$$log\,10\,pr \sim normal(\mu, \sigma \mid \mu_0, \sigma_0, \alpha, \beta, T, N)$$

where $T$ is the smoothed GMST, $N$ is the Nino3.4 for OND, $\mu_0$ and $\sigma_0$ are the mean and variance parameters of the nonstationary distribution and $\alpha$, $\beta$ are the trends due to GMST and Nino3.4, respectively. Maximum likelihood estimation is used to estimate the model parameters, with

$$\mu = \mu_0\, exp\left(\frac{\alpha T + \beta N}{\mu_o}\right) \text{ and } \sigma = \sigma_0\, exp\left(\frac{\alpha T + \beta N}{\mu_o}\right).$$

This formulation is used to ensure that the distribution has fixed dispersion. For attribution, the distribution is evaluated with $N$ fixed at the 2022 value in both the current and 1.2 °C cooler climate distributions, in order to obtain the change in likelihood and intensity of the 2022 OND low rainfall event due to climate change under the 2022 Nino conditions. For MAM, we only fit log10(precip), which depends on GMST.

## 3. Results and discussions

### 3.1. Observational analysis

#### 3.1.1. MAM precipitation

Fig. 2 shows the trend-fitting results for MAM precipitation in CPC and CenTrends-CHIRPS. Fig. 2a and c shows the log-transformed variable as a function of the GMST anomaly, while Fig. 2b and d shows the return period curves for the log-transformed variable in the 2022 climate (red lines) and 1.2 °C cooler climate (blue lines). While there is a tendency towards decreasing rainfall with GMST rise in both datasets, the trend is stronger in CPC. Similar trends are obtained when the datasets are truncated to have the same length (see Supplementary Material Fig. S7). The best estimates of the return period of the 2022 event are 11 and 6 years for CPC and CenTrends-CHIRPS, respectively. We round these to an average of 10 years for the attribution analysis. The 2022 MAM rainfall deficit is found to be 7 times (uncertainty: 0.2 to 3 600) and 2 times (uncertainty: 0.4 to 8) more likely in the 2022 climate, from the CPC and CenTrends-CHIRPS datasets, respectively. The respective intensity changes are −26% (uncertainty: 60%–25%) and −8% (uncertainty: 31%–17%), implying that the 2022 MAM rainy season was drier due to climate change.

#### 3.1.2. OND precipitation

In Section 2.5.2, we noted that the OND rainy season is known to be affected by the ENSO. To test whether the detrended OND Niño3.4 index should be included in the attribution analysis, we fit a simple linear regression to the log-transformed precipitation: once using only GMST as the explanatory variable (Model 1), and again including Niño3.4 as an additional covariate (Model 2). The estimated coefficients for each model are shown in Table 1, with those coefficients that were found to be statistically significant at the 5% level bolded and marked with an asterisk. In Model 1, the trend in GMST was not found to be statistically significant in either dataset; in Model 2, when the effect of Niño3.4 was taken into account, a stronger linear trend in GMST was identified. The linear relationship between Niño3.4 and OND precipitation was found to be statistically significant in both datasets, and the inclusion of the effect also revealed a statistically significant trend in GMST in the CenTrends-CHIRPS dataset. Fig. 3 shows the fitted trends for each model; the weaker trends in the GMST-only model are evident. The difference in the models is possibly due to confounding effects of ENSO on the GMST trend: in particular, the occurrence of three consecutive La-Niña years at the end of the time series masks the underlying GMST trend to some extent.

We therefore decided to include the effect of OND Niño3.4 as a covariate in the statistical model used in the attribution analysis for OND precipitation. In order to focus on the change in GMST, we fix the Niño3.4 covariate at the 2022 level and only report the effect of increasing GMST on OND precipitation levels. Fig. 4 shows trend-fitting results for OND precipitation, conditioned on the 2022 OND Niño3.4 (see Section 2.5.2 for details). Both datasets provide evidence of an increasing trend in the observations of OND precipitation in this region (Fig. 4a and c). Similar results are obtained when the datasets are truncated to have the same length (see Supplementary Material Fig. S7). The return period of the 2022 event in the current climate is estimated at 7 and 3 years in the CPC and CenTrends-CHIRPS datasets, respectively (right-hand panels in Fig. 4), which are averaged to 5 years for the attribution analysis. The best estimates for the PR are less than 1 in both datasets, with PR = 0.3 (uncertainty: 0.06 to 2) in CPC and PR = 0.5 (uncertainty: 0.2 to 1) in CenTrends-CHIRPS, suggesting that drought in

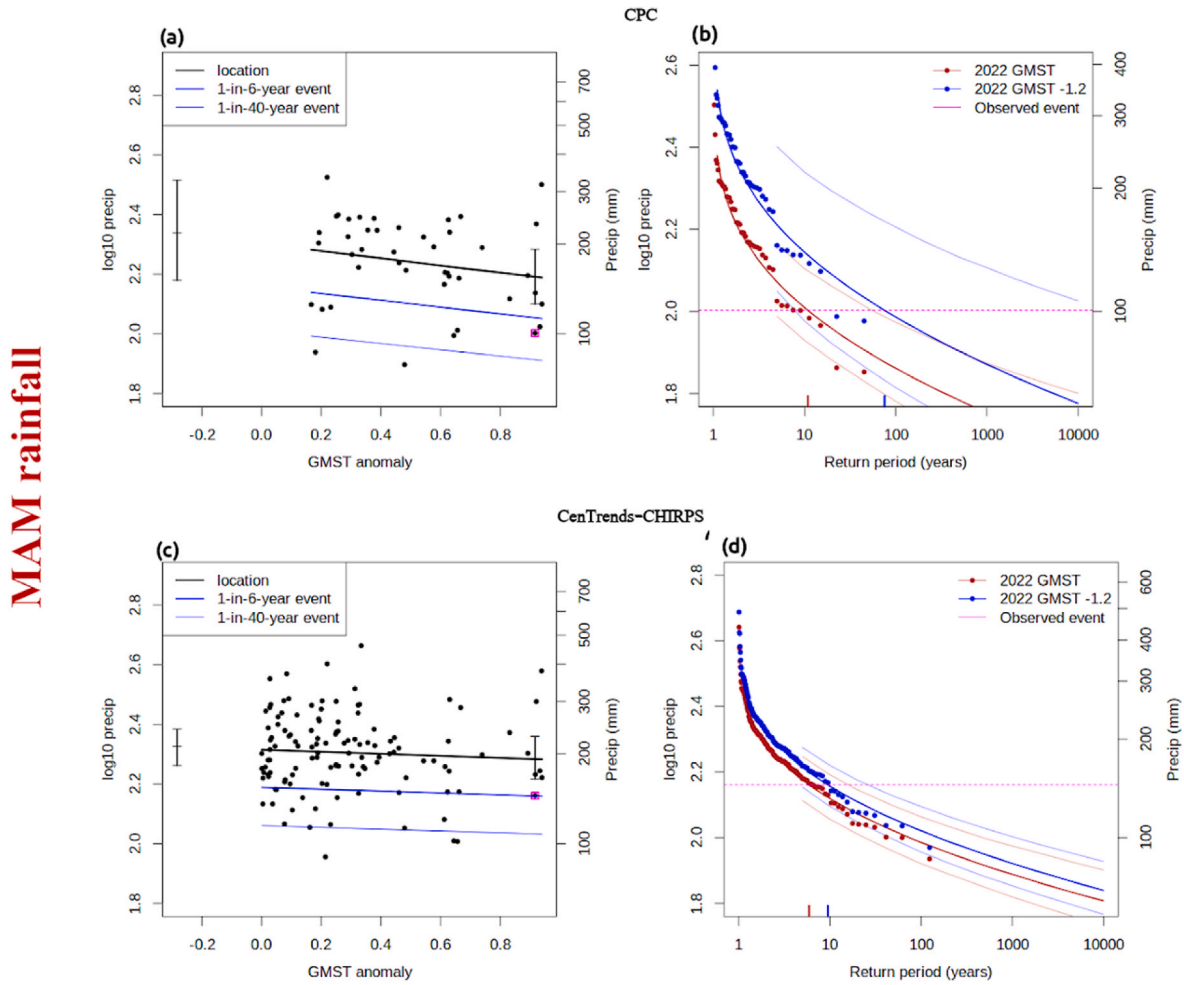


**Fig. 2.** Left: Response of MAM rainfall (log-transformed) to change in GMST, based on the CPC (**a**) and CenTrends-CHIRPS (c) datasets. The thick black line denotes the time-varying mean, and the blue lines show 6- and 40-year return levels. The vertical black lines show the 95% confidence interval for the location parameter, for the 2022 climate and the hypothetical, 1.2 °C cooler climate. The 2022 observation is highlighted with the magenta box. Right: Gaussian return periods of log-transformed rainfall for the 2022 climate (red lines with 95% CI) and a 1.2 °C cooler climate (blue lines with 95% CI) for CPC (**b**) and CenTrends-CHIRPS (d) datasets.

**Table 1**
Fitted coefficients from linear models of log10precip with GMST only (Model 1) as covariate and both GMST and Niño3.4 as covariates (Model 2) for the short rains. Significant coefficients at 5% level are marked with * and highlighted in bold.

| Dataset | Model 1: GMST only | Model 2: GMST & Nino |
|---|---|---|
| CPC | 0.1704 | 0.3253 & **0.1878*** |
| CenTrends-CHIRPS | 0.2439 | **0.3107*** & **0.189*** |

the short rain season has been made less likely due to climate change but without statistical significance. The intensity changes also suggest that OND precipitation has increased by around 39% (CPC, uncertainty: 17%–121%) and 30% (CenTrends-CHIRPS, uncertainty: 3%–70%).

### *3.1.3. 24-Month precipitation and SPEI*

Fig. 5 shows the trends for the mean 24-month precipitation over the study region. The CPC dataset shows a decreasing trend (Fig. 5a) while in the CenTrends-CHIRPS dataset the trend slightly increases (Fig. 5c). While these results are based on different data lengths of these datasets (44 years of CPC and 122 years of CenTrends-CHIRPS), equal lengths of data show the same results (see Supplementary Material Fig. S7). The difference between the two datasets could partly be explained by opposed trends MAM (increase) and OND (decrease) rainfall (see Figs. 2 and 4); with CPC showing stronger decreasing trends in OND. Fig. 5b and d shows the return period curves for the variable in the current 2022 climate and a hypothetical 1.2 °C cooler climate. The best estimate of the return period for the 24-month low precipitation event ending in 2022 is found to be roughly 20 years in both datasets. The event is found to have been made 2 times more likely (uncertainty: 0.1 to 360) and 7% drier (uncertainty: 31% drier to 21% wetter) by climate change in the CPC dataset (Fig. 5b). The results based on CenTrends-CHIRPS dataset (Fig. 5d), on the other hand, show the meteorological drought to have become less likely (PR = 0.7 uncertainty: 0.1 to 5) and 3% wetter (uncertainty: 12% drier to 19% wetter). It is noted that the uncertainties are high around these estimates and that the uncertainties from the two datasets overlap.

Fig. 6 shows trend-fitting analysis for SPEI using the CPC dataset; SPEI cannot be computed for CHIRPS-CenTrends, which does not provide temperature data. The 2022 observed SPEI value in the CPC dataset is −2.6, corresponding to an exceptional drought; the return period of this event in the current climate is about 10 years. The climate change signal is much stronger, with the event made 5 500 times (uncertainty: 32 to 4e+08) more likely and made more severe by 2.4 SPEI units (uncertainty: 4.7 to −1.2); in other words, in this model a 1-in-10 year drought event in a world without climate change would be expected to have an SPEI of 0.3 (uncertainty: 1.4 to 2.1), corresponding to normal conditions with respect to the 1980–2010 climatology or, in the worst case, a drought classification of D0 (abnormally dry conditions).

Fig. 7 shows the joint distribution of the 24-month precipitation and

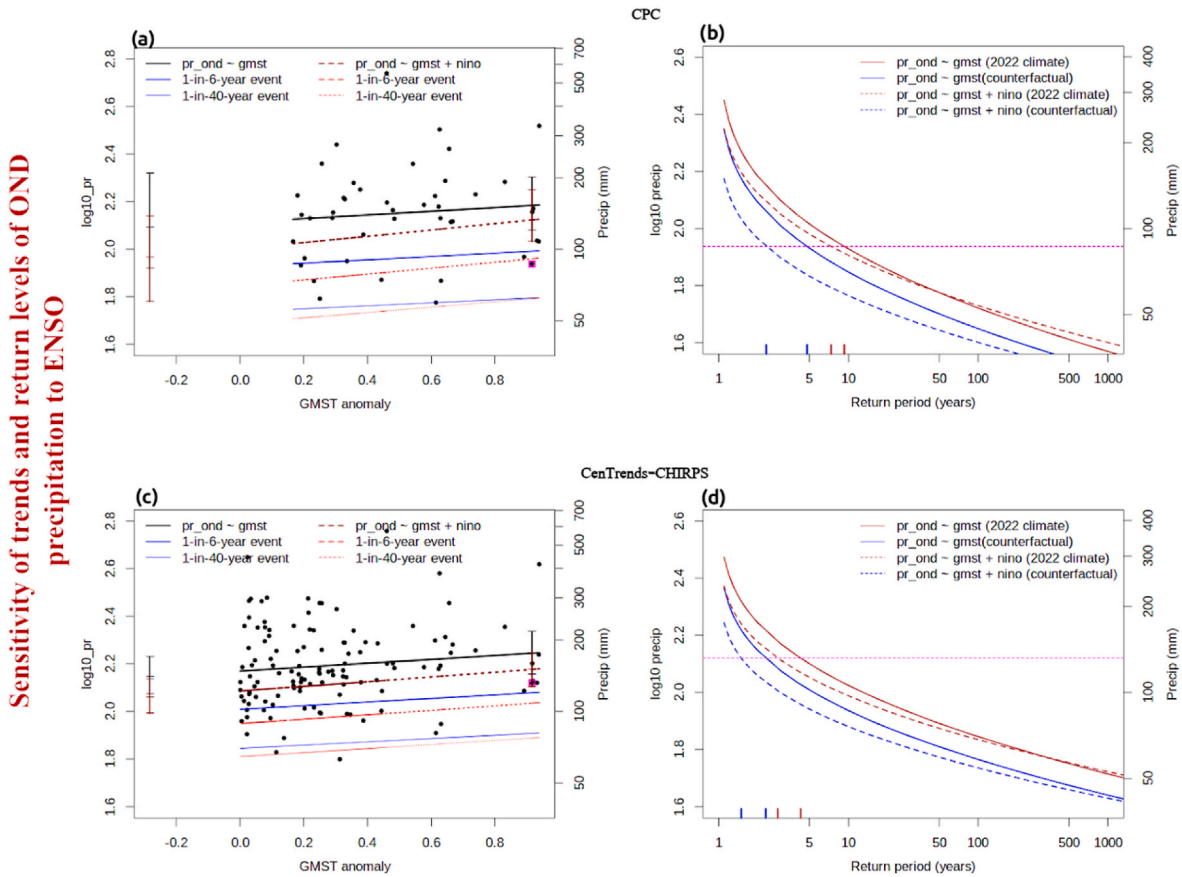


**Fig. 3.** Comparison between fitted models for OND rainfall using only GMST as a covariate and using both GMST and the detrended Niño3.4 index as covariates. Left: Linear trend as a function of GMST only (solid black and blue lines) and as a function of GMST with the detrended Niño3.4 (dotted black and blue lines) index fixed at the 2022 value based on the CPC (**a**) and CenTrends-CHIRPS (**c**) datasets. Right: Gaussian return levels of log-transformed rainfall for the 2022 climate (red lines) and a 1.2 °C cooler climate (blue lines) based on the CPC (**b**) and CenTrends-CHIRPS (d) datasets. Solid lines indicate return levels for the standard model depending only on GMST; dashed lines show return levels depending on GMST and the detrended Niño3.4 index, with Niño3.4 fixed at the 2022 level. Observed points and confidence intervals are not shown to avoid obscuring the comparison between the estimated return levels.

PET, along with the corresponding SPEI drought classification for each pair of values. The joint contours show that the probability of this particular combination of precipitation and PET in any given year in the 2022 climate is 1 in 26. The plot also highlights how unlikely the event would have been to occur in a 1.2 °C cooler climate, with the magenta point marking the 2022 event lying very far from the dashed contours representing the joint distribution in a cooler climate.

### 3.2. Hazard synthesis: multi-method multi-model attribution

For models that pass the evaluation test (see section 2.4), we calculate Probability Ratios (PR) and change in intensity (ΔI) for 24-month, 2022 MAM and OND rainfall, and 24-month SPEI. See Supplementary Material Tables S5–S7 for the results. In this section, we synthesise PR and ΔI results for the selected climate models along with observations-based products to obtain an overarching attribution statement. Figs. 8a–11a show bars for the changes in probability (left-hand side) and intensity (right-hand side) for the observations (blue) and models (red) in the 2022 climate versus a 1.2 °C cooler climate representing the pre-industrial world. Figs. 8b–11b show the changes in the 2022 climate versus a future climate 0.8 °C warmer than 2022 (2 °C warmer than the pre-industrial climate). The best estimate for each dataset is marked with a black triangle.

In this synthesis, we first add a representation error (in quadrature) to the observations to account for the difference between observation-based datasets that cannot be explained by natural variability. This is shown in these Figures as white boxes around the light blue bars. The dark blue bar shows the average over the observation-based products. Next, a term to account for inter-model spread is added (in quadrature) to the natural variability of the models. This is shown in the Figures as white boxes around the light red bars. The dark red bar shows the model average, consisting of a weighted mean using the (uncorrelated) uncertainties due to natural variability. Observation-based products and models are combined into a single result in two ways. Firstly, we neglect common model uncertainties beyond the inter-model spread that is depicted by the model average and compute the weighted average of models (dark red bar) and observations (dark blue bar) — this result is shown by the magenta bar. To account for the fact that, due to common model uncertainties, model uncertainty can be larger than the inter-model spread, we also show the more conservative estimate of an unweighted direct average of the observations (dark red bar) and models (dark blue bar) contributing 50% each, indicated by the white box around the magenta bar in the synthesis Figures.

The model results largely replicate those in the observations, namely showing an increase in the likelihood and intensity of a 1 in 10-year dry event for MAM, a decrease in the likelihood and intensity of a 1 in 5-year dry event for the OND, no change for the 1 in 20-year dry event in the 24 months rainfall and strong increase in the likelihood and intensity for SPEI. While a small number of individual models show different changes, leading to large uncertainties and statistically insignificant results, on average the models and observations show very similar changes, quantitatively and qualitatively. These results can be summarised as roughly a doubling in likelihood for the low MAM rains (Fig. 8a; left) with about 11% less rainfall (Fig. 8a; right), although the

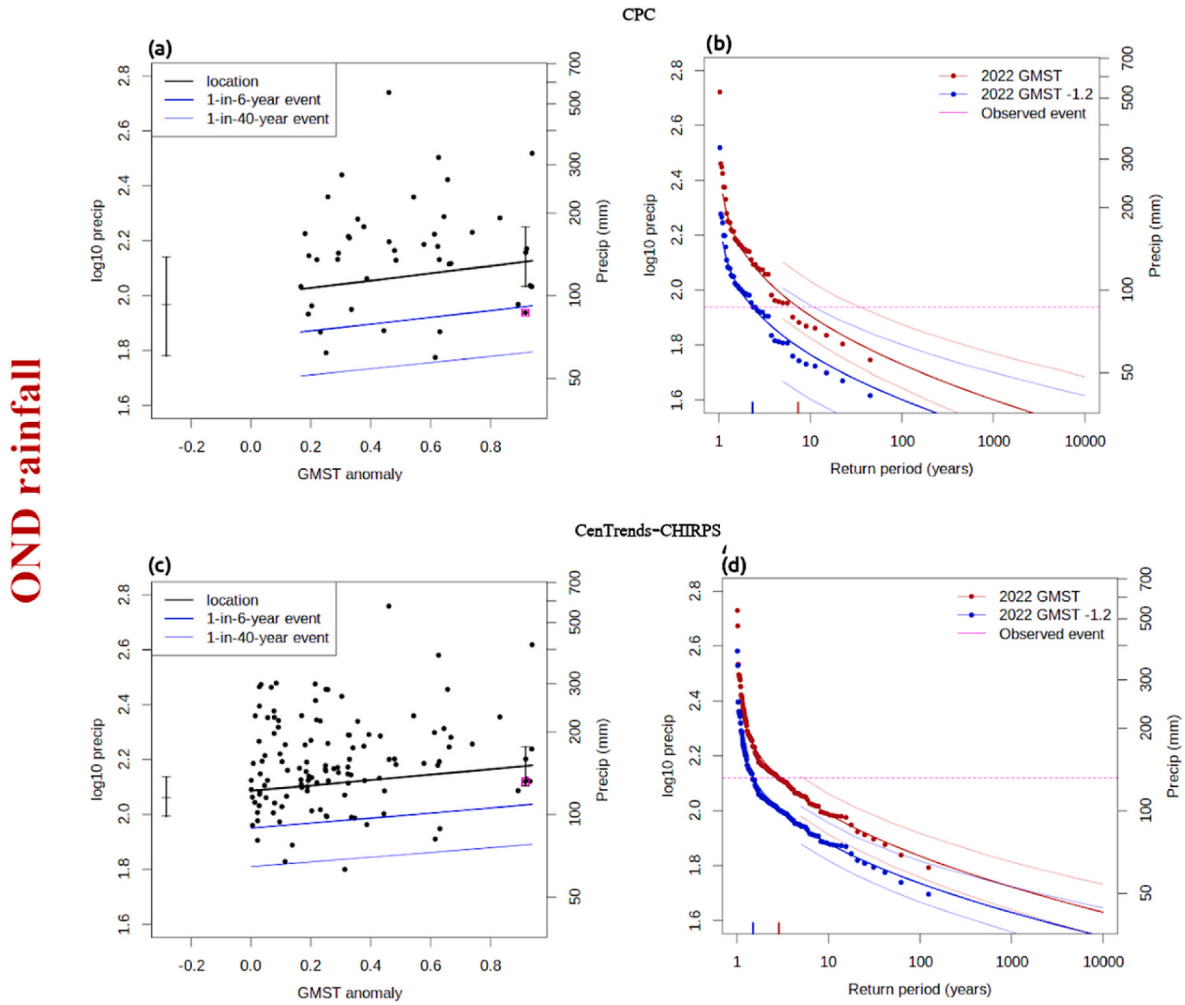


**Fig. 4.** Left: Response of OND rainfall (log-transformed) to change in global mean temperature, based on the CPC (**a**) and CenTrends-CHIRPS (**c**) datasets. The thick black line denotes the time-varying mean, and the blue lines show 6- and 40-year return levels. The vertical black lines show the 95% confidence interval for the location parameter, for the 2022 climate and the hypothetical, 1.2 °C cooler climate. The 2022 observation is highlighted with the magenta box. Right: Gaussian return periods of log-transformed rainfall for the 2022 climate (red lines) and the 1.2 °C cooler climate (blue lines) in the CPC (**b**) and CenTrends-CHIRPS (**d**) datasets, with 95% confidence intervals shown by fainter lines of the same colours.

uncertainty ranges encompass no change. For the OND, when using the NINO3.4-index as an additional covariate as described in section 3.1.2, the likelihood of low rains decreased by about a factor of five (Fig. 9a; left) and rainfall intensity increased by approximately 25 % (Fig. 9a; right).

The 24-month SPEI, combining the effects of precipitation changes and temperature-driven evapotranspiration, shows a very strong increase in the likelihood and intensity of the 1 in 20-year drought event (Fig. 11). As is often the case with temperature-related indices (Van Oldenborgh et al., 2022) the increase in likelihood and intensity in the observations is much larger than in the models, rendering the synthesised results, which show an increase in likelihood of a factor of about 100, conservative (Fig. 11a). Due to the likely sensitivity of the SPEI to both the choice and length of dataset and the method used to compute the PET, we carried out a sensitivity analysis to understand the likely impact on the results presented here (see Supplementary Material Fig. S5). Due to the absence of temperature data in CenTrends-CHIRPS, we were unable to compute PET for this dataset; instead, we compared the results for CPC with the same analysis for the ERA5 dataset. For ERA5, we used both pre-calculated (based on Penman–Monteith) and calculated (based on Thornthwaite, Hargreaves and Baier-Robertson) PET estimates. Plots of the fitted return levels and decomposition of the 24-month SPEI into the contributions from PET and precipitation, and drought classifications are provided in Supplementary Material Figs. S8 and S9. Thornthwaite classified the drought as exceptional (drought class D4) in the current climate and normal (not in a drought class) in 1.2 °C cooler climate in both datasets. Based on the CPC dataset, the 2021–2022 SPEI was classified as exceptional (drought class D4) in both the 2022 and 1.2 °C cooler climates when using both Baier-Robertson and Hargreaves, but with a higher severity in 2022. In ERA5, the event was classified as moderate (drought class D1) in 1.2 °C cooler climate and exceptional (drought class D4) in 2022 when using Baier-Robertson, while Hargreaves deemed it severe (drought class D3) in the past and exceptional (drought class D4) in the present. As expected, the differences between the methods and datasets influence the drought classification through the varied data inputs and climatic conditions in the PET estimates (refer to section 2.2 for details). However, even with ERA5 PET, which is based on the Penman–Monteith method that accounts for radiative and aerodynamic processes, we observed similar SPEI trends compared to the temperature-based estimates. Overall, both datasets show an increased tendency towards severe drought conditions with rising GMST, regardless of the PET estimation method used. These results are corroborated when looking at the same event definitions in the future — in a 0.8 °C warmer climate (Fig. 11b), although the projected changes are much smaller compared with the changes from the past up to now. This could be partly due to the future

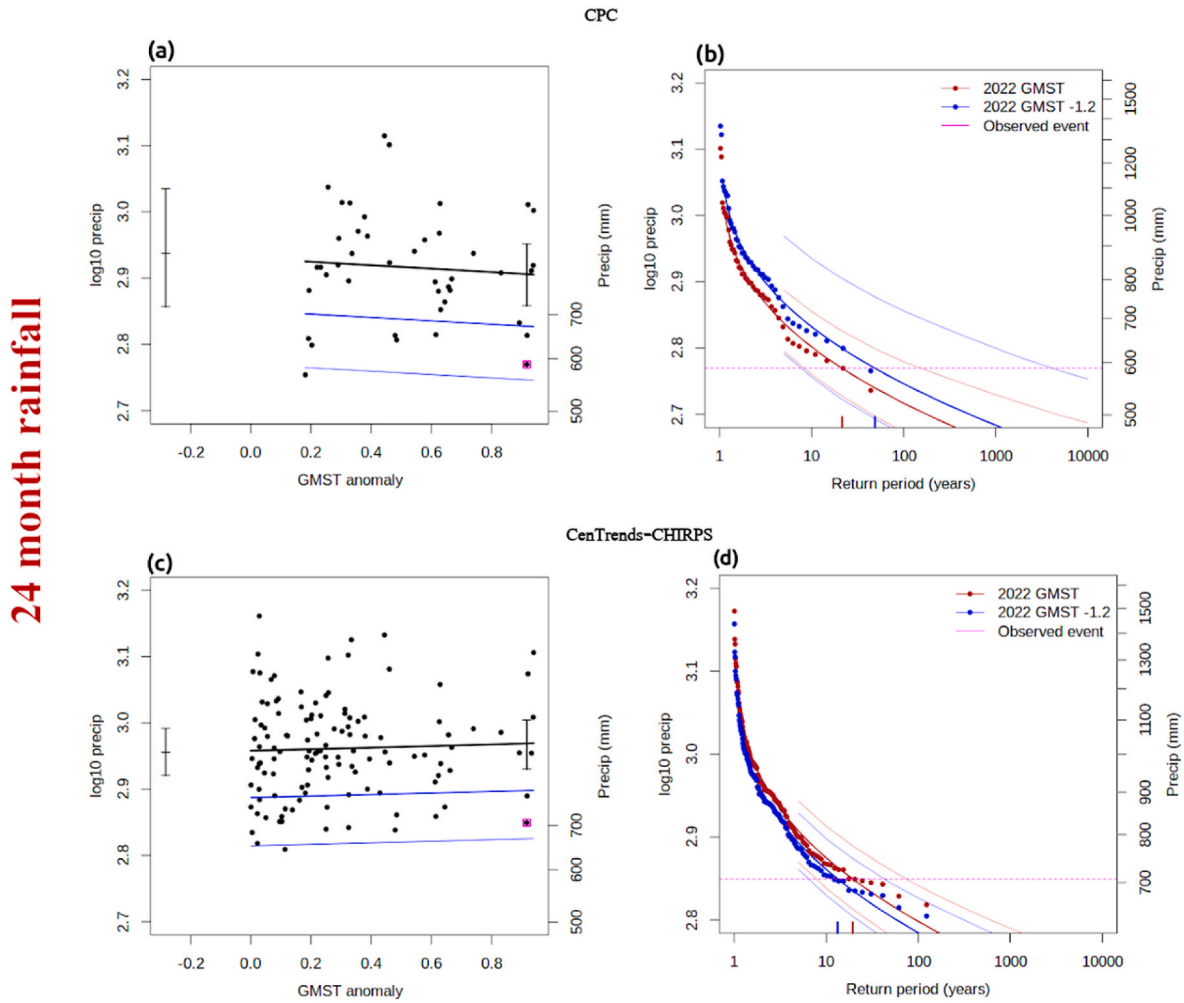


**Fig. 5.** Left: Response of 24-month rainfall (log-transformed and averaged over the study region) to change in global mean temperature, based on the CPC (**a**) and CenTrends-CHIRPS (**c**) datasets. The thick black line denotes the time-varying mean, and the blue lines show 1 standard deviation (s.d) and 2 s d below. The vertical black lines show the 95% confidence interval for the location parameter in the 2022 climate and the hypothetical 1.2 °C cooler climate. The average 24-month rainfall from Jan 2021–Dec 2022 is highlighted with the magenta box. Right: Gaussian-based return periods of log-transformed rainfall for the 2022 climate (red lines) and the 1.2 °C cooler climate (blue lines with 95% CI), based on CPC (**b**) and CenTrends-CHIRPS **(d)** datasets.

wetting trend in the region indicated by models (Rowell et al., 2016). Combining lines of evidence from the synthesis results of the past climate, results from future projections and physical knowledge, we conclude that the drought severity has increased dramatically because of human-induced climate change. This is primarily driven by the strong increase in temperature and thus PET, but there is also evidence that this is augmented by drying of the long rains.

## 4. Context of the event

While the changing frequency and intensity of droughts discussed in Section 3.2 are important factors in the impacts described in Section 1, these impacts occur through the confluence of hazard with vulnerability and exposure factors (IPCC, 2012; Raju et al., 2022; Thalheimer, 2023). Having a holistic understanding of vulnerability and exposure can avoid blaming climate for all disasters and can help reduce maladaptation that comes from reinforcing existing inequities (Eriksen et al., 2021; Otto and Raju, 2023). Here, we present the historical context for the current drought, then provide the larger drivers of vulnerability followed by drought management and response practices. Finally, bringing together the vulnerability and exposure factors with the findings of the attribution study, we offer a vulnerability analysis that aims to provide tools for reducing future drought impacts, and future research directions.

### 4.1. *Chronic drought exposure*

The Horn of Africa (HoA) experiences recurring drought conditions that have been hypothesised to be connected to climate change (Funk, 2020; Funk et al., 2019). The disaster database, (EM-DAT) summarises the impacts of various natural hazards from 1964 onwards, and records 17–18 drought events for the countries in the study region (see Table 2) – a likely underestimate given known gaps in the data, and one that does not account for drought years prior to 1964 (EM-DAT).

The length of the current drought – five consecutive seasons of below-average rainfall – is unprecedented in the reliable rainfall record, which extends back to 1950 (Climate Hazards Center, 2023). The consecutive nature of these failed rainy seasons drove the high level of impacts experienced, as most people may be able to deal with one or two failed seasons, but more than that stretches their resources and tests their ability to cope. For example, warnings of possible famine in Somalia after several failed rainy seasons were given and, while the official threshold for Famine declaration (IPC Phase 5) has been avoided with increased government and humanitarian aid, there has been excess mortality associated with hunger and acute malnutrition occurring concurrently with disease outbreaks (FEWS NET, 2022). Significant interannual and seasonal variability in rainfall in the region has also created back-to-back cycles of flooding and drought that negatively affects coping capacity (Nicholson, 2016, 2017; Palmer et al., 2023). The

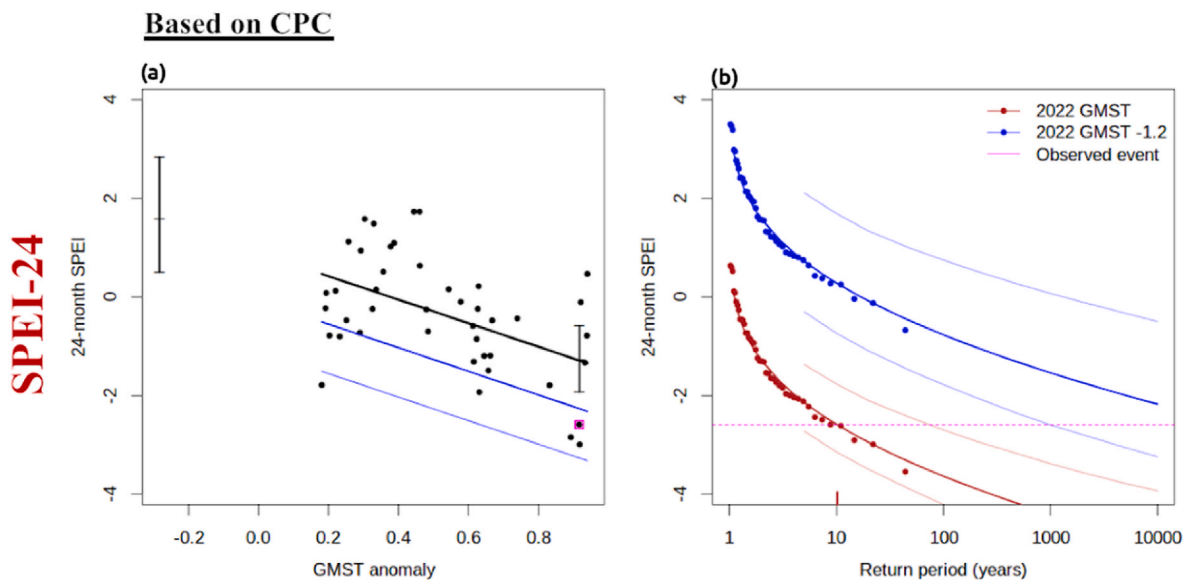


**Fig. 6. (a)** Response of SPEI-24, computed from CPC mean 24-month precipitation and mean 24-month PET over the study region, to change in global mean temperature. The thick black line denotes the time-varying mean, and the blue lines show 6- and 40-year return levels. The vertical black lines show the 95% confidence interval for the location parameter, for the current climate and a hypothetical 1.2 °C cooler climate. The 2022 observation is highlighted with the magenta box. **(b)** Gaussian-based return periods of log-transformed rainfall for the 2022 climate (red lines) and a 1.2 °C cooler climate (blue lines) with 95% CI, based on CPC dataset.

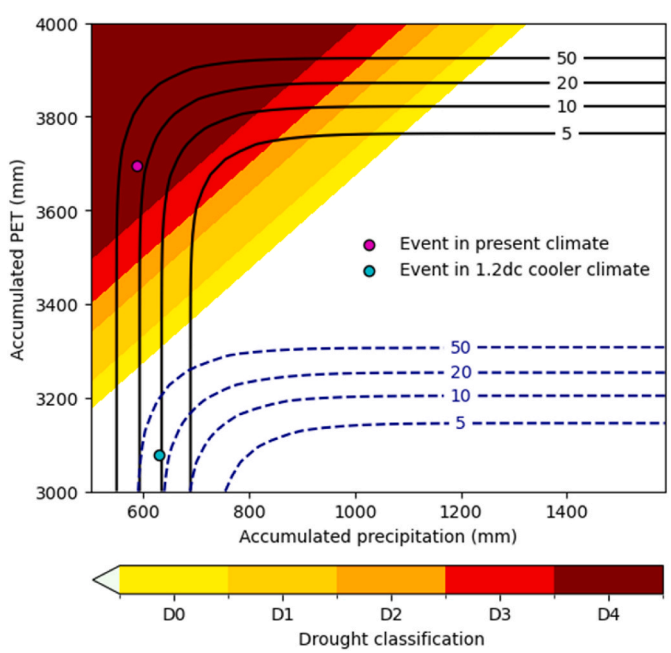


**Fig. 7.** Joint distribution of 24-month precipitation and PET with corresponding SPEI drought classification (CPC dataset). The solid contours indicate return periods under the joint distribution in the current climate, while the dashed contours indicate the same return periods in a 1.2 °C cooler climate. The shaded contours represent different levels of drought severity. The magenta point indicates the 2022 drought event in the 2022 climate, with this particular combination of precipitation and PET having a joint return period of 26 years, while the turquoise point shows an event of equivalent rarity in a 1.2 °C cooler climate.

March to May 2020 season directly before the beginning of this drought was exceptionally wet and resulted in floods that killed hundreds of people and displaced hundreds of thousands. The current drought is also driving internal displacement, which can increase pre-existing and structural vulnerability, especially of women to gender-based violence, and health risks associated with crowded camps (FEWS NET, 2023). Other compounding factors, including locust outbreaks in 2019–2022 that reduced crop yields, rising global food prices, COVID-19 and the government response all provide a backdrop against which the drought occurred (Thalheimer, 2023).

### 4.2. *Drivers of vulnerability and exposure*

#### 4.2.1. *Environmental degradation and land-use changes*

Over the past decades several factors including environmental degradation, unsustainable land-use practices and harvesting, the overexploitation of grazing land and other pastoral activities, and deforestation, have impacted ecosystems and increased vulnerability of local communities (Prieto-Garcia et al., 2022; Tache, 2013). Several indigenous plants have been declining, including the Yeheb plant, a small tree endemic to the drylands of Ethiopia and Somalia which contains high nutritional and economic value (Prieto-Garcia et al., 2022). The importance of smallholder farmers, pastoralists, ranchers, and local communities to effectively use their own land remains greatly undervalued, and remains marginalised due to inadequate legislative protection, urbanisation, and private investments promoted by the government (Tache, 2013; Tura, 2018). Insecure land rights are exacerbated by the unprecedented acquisition of land by international agro businesses (World Bank, 2013). In Ethiopia, a large number of foreign investors are leasing millions of hectares with licences for commercial farms (Graham et al., 2009; Tache, 2013). Across the Maasai land, pastoral land has been lost, often gradually, with smaller amounts of land being taken by wealthier herders or transferred to outsiders who seek title-deeds as collateral for loans or long-term investments (Homewood et al., 2009; Rutten, 1992; Tache, 2013). Furthermore, the development of hydropower plants is known to drive land dispossession, such as in Ethiopia during the development of the Gibe III dam (Schapper et al., 2020). The loss of access to traditional grazing lands and water sources has had devastating effects on pastoralist communities, who rely on mobility and flexibility to manage their herds during times of drought (Lwanga-Ntale and Owino, 2020). Lastly, the large influx of refugees into Kenya over the years has increasingly stretched the few resources available, contributing further to environmental degradation (OCHA, 2023b).

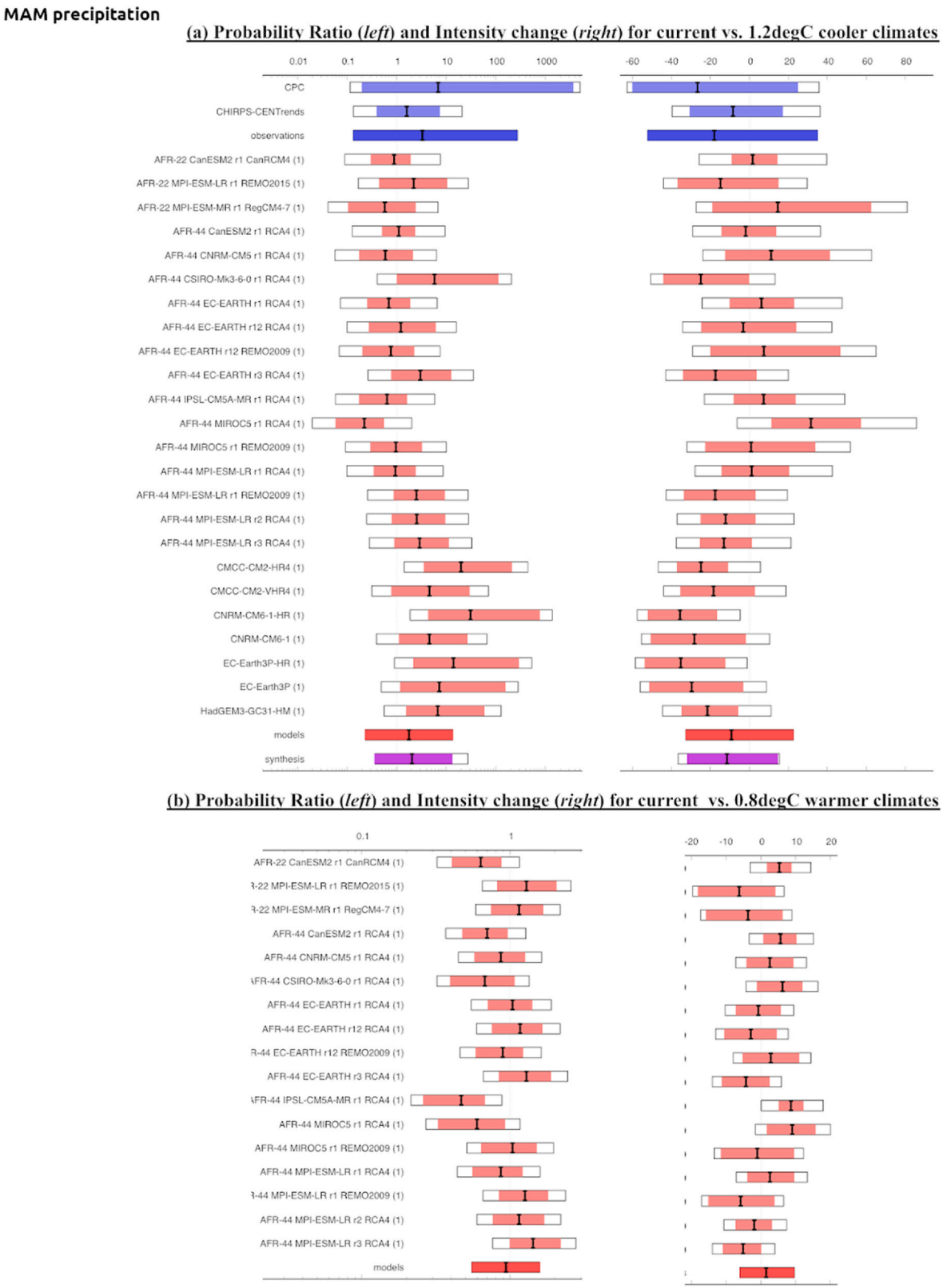


**Fig. 8.** (**a**) Synthesis of probability ratios (left) and intensity changes (%; right) when comparing the return period and magnitudes of the MAM rainfall over EA in the current climate and a 1.2 °C cooler climate. (**b**) Same as (**a**) in the current climate and a future 0.8 °C warmer climate.

### *4.2.2. Conflict and fragility*

East Africa has a longstanding history of conflict and fragility directly affected by socioeconomic and political drivers and indirectly by climate variability (Owain and Maslin, 2018). Conflict and insecurity exacerbate environmental and natural resource challenges (Krieger et al., 2020; Thalheimer and Webersik, 2021; World Bank, 2020). Recurring extreme wet and dry events across the region have also contributed to fragile livelihood outcomes including internal displacement (Thalheimer et al.,

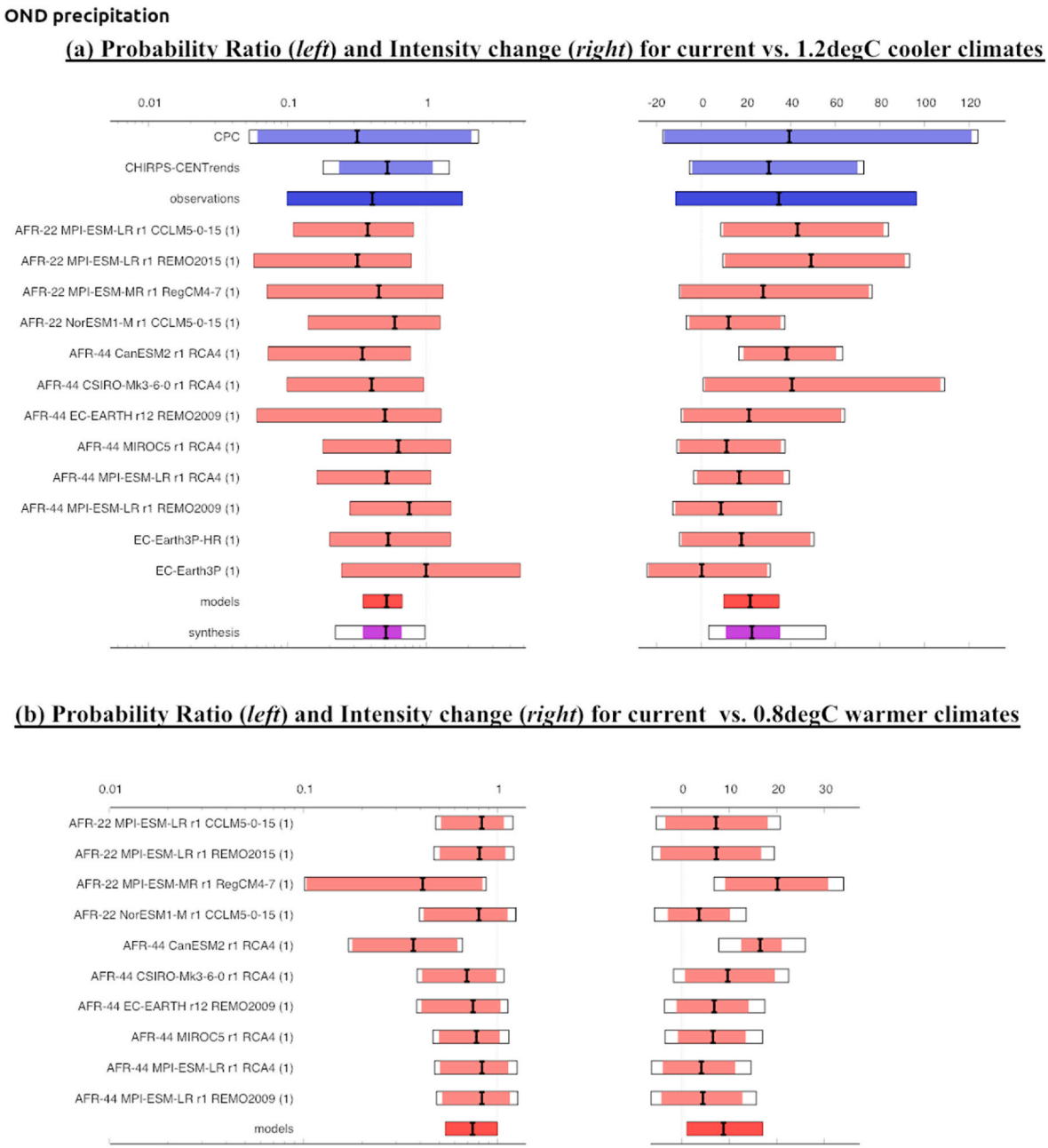


**Fig. 9.** **(a)** Synthesis of probability ratios (left) and intensity changes (%; right) when comparing the return period and magnitudes of the OND rainfall over EA using NINO3.4 as an additional covariate in the current climate and a 1.2 °C cooler climate. (**b**) Same as (**a**) in the current climate and a future 0.8 °C warmer climate.

2023). Drought and water insecurity have been linked to increased social competition in arid and semi-arid regions, especially for pasture and water (Meier et al., 2007; Von Uexkull et al., 2016). Despite rapidly growing empirical evidence on the links between climate and conflict (Koubi, 2019; Von Uexkull & Buhaug, 2021), analytical challenges remain in the detection and attribution of these links due to the multi-causality of conflict and associated impacts (Buhaug et al., 2023). The drought has internally displaced more than 1.4 million people since 2021, 1.1 of whom were displaced over the course of 2022 (UNHCR, 2023b).

Conflict and fragility conditions in the presence of weather and climate-related events vary across countries in the HoA region (Thalheimer et al., 2021). Somalia faces one of the most complex challenges of any country in the world more than 30 years after the state collapsed (Waaben Thulstrup et al., 2020). Civil war and the presence of armed conflict groups hamper efforts of state-building and peace. During the 2021-22 drought period many Somalis lost their livelihoods, which led to soaring food prices and their coping capacities were stretched too thinly to recover. Others crossed the border to seek help in Kenya and Ethiopia, joining a large existing refugee population. Fig. 12 shows priority needs of drought and conflict-affected internally displaced people (IDP) in Somalia from Jan 2016 to Dec 2022 - spikes in 'Food' needs can be seen in 2021 and 2022 in response to both conflict and drought. Women and children make up over 80 percent of Somalia's drought-displaced population (Mason et al., 2012; UNHCR, 2023d) these compound vulnerabilities have exacerbated protection risks and pre-existing inequities (Thalheimer, 2023; Thalheimer et al., 2021a,b).

### 4.2.3. *Social vulnerability*

Socioeconomic deprivation increases exposure and vulnerability to shocks such as the 2021-22 drought, it simultaneously decreases communities' abilities to invest in adaptation and risk reduction measures

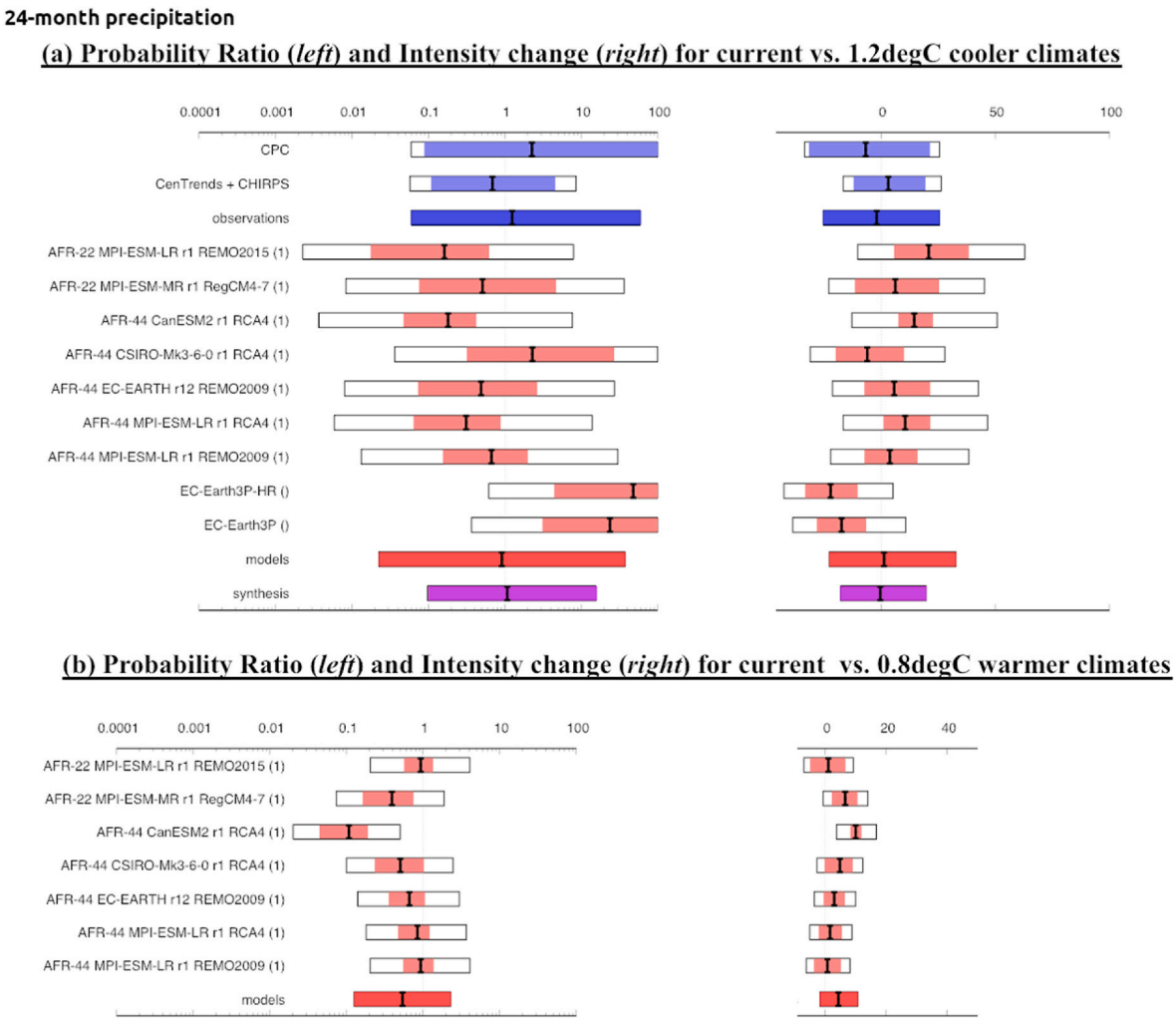


**Fig. 10.** (**a**) Synthesis of probability ratios (left) and intensity changes (%; right) when comparing the return period and magnitudes of the 24-month precipitation from 2021 to 2022 over EA in the current climate and a 1.2 °C cooler climate. (**b**) Same as (**a**) in the current climate and a future 0.8 °C warmer climate.

(Hill and Porter, 2017). The HoA region is home to a considerable number of people facing chronic food and water insecurity, malnutrition, and limited access to basic services including infrastructure, health care, education, and social protection systems (OHCHR, 2020; Prieto-Garcia et al., 2022; UNDP, 2022). The impacts differ by country depending on local vulnerability and exposure factors, with Somalia's fragility particularly limiting people's ability to meet basic needs, driving displacement and increased mortality (FEWS NET, 2022). Studies highlight malnutrition and an increase in incidence of risk of diarrheal diseases such as cholera (Asmall et al., 2021), infant mortality (WHO, 2023) menstrual and maternal complications (OCHA, 2023b) during drought episodes in HoA. Roughly half the population in Somalia and Ethiopia have limited access to energy (Our World in Data, 2022a; 2022b) with many rural communities across all three countries having limited access to electricity (Getie, 2020; Njiru and Letema, 2018). Households engaged in climate-sensitive livelihoods like rainfed agriculture, agropastoralism, and pastoralism are notably vulnerable to drought and are among the most severely impacted (Bogale and Erena, 2022; Pape and Wollburg, 2019; Thomas et al., 2019; Yayeh Ayal et al., 2022). The poorest in the community and elderly people, notably older women, are disproportionately vulnerable (Omolo and Mafongoya, 2019). Evidence suggests that drought is the natural hazard most closely associated with poverty (Shepherd et al., 2015). With the recurrent extreme climate conditions experienced in recent years, households have been forced to spend their limited assets on buffering losses and damages, consequently pushing them into a poverty trap (Pape and Wollburg, 2019; Sherwood, 2013; World Bank, 2019).

### 4.3. Drought management and response

#### 4.3.1. Institutional capacity

The impacts of droughts can be mitigated by policies, coping strategies, early warning and early action. IGAD Climate Prediction and Applications Centre (ICPAC) provides seasonal regional climate outlooks. At the national level, each country in the region has a national hydro meteorological agency. While the five failed seasons were well forecasted and timely warnings issued (e.g. see ICPAC seasonal forecasts and FEWSNET East Africa bulletins; KMD 2022), drought management policy and coordination in the three affected countries differs significantly, putting them at different starting points to respond. In HoA, drought response generally happens at multiple levels. Ideally, national governments and their devolved levels of jurisdiction would organise the response led by different sectors and agencies. In situations where national capacity is overwhelmed, humanitarian response mechanisms are meant to fill the gaps. In reality, these lines can be less clear, particularly in situations where there is already a significant humanitarian and development presence, as there is in the HoA at the time of writing.

The Kenyan National Drought Management Authority (NDMA, 2016), is mandated to carry out activities related to drought risk

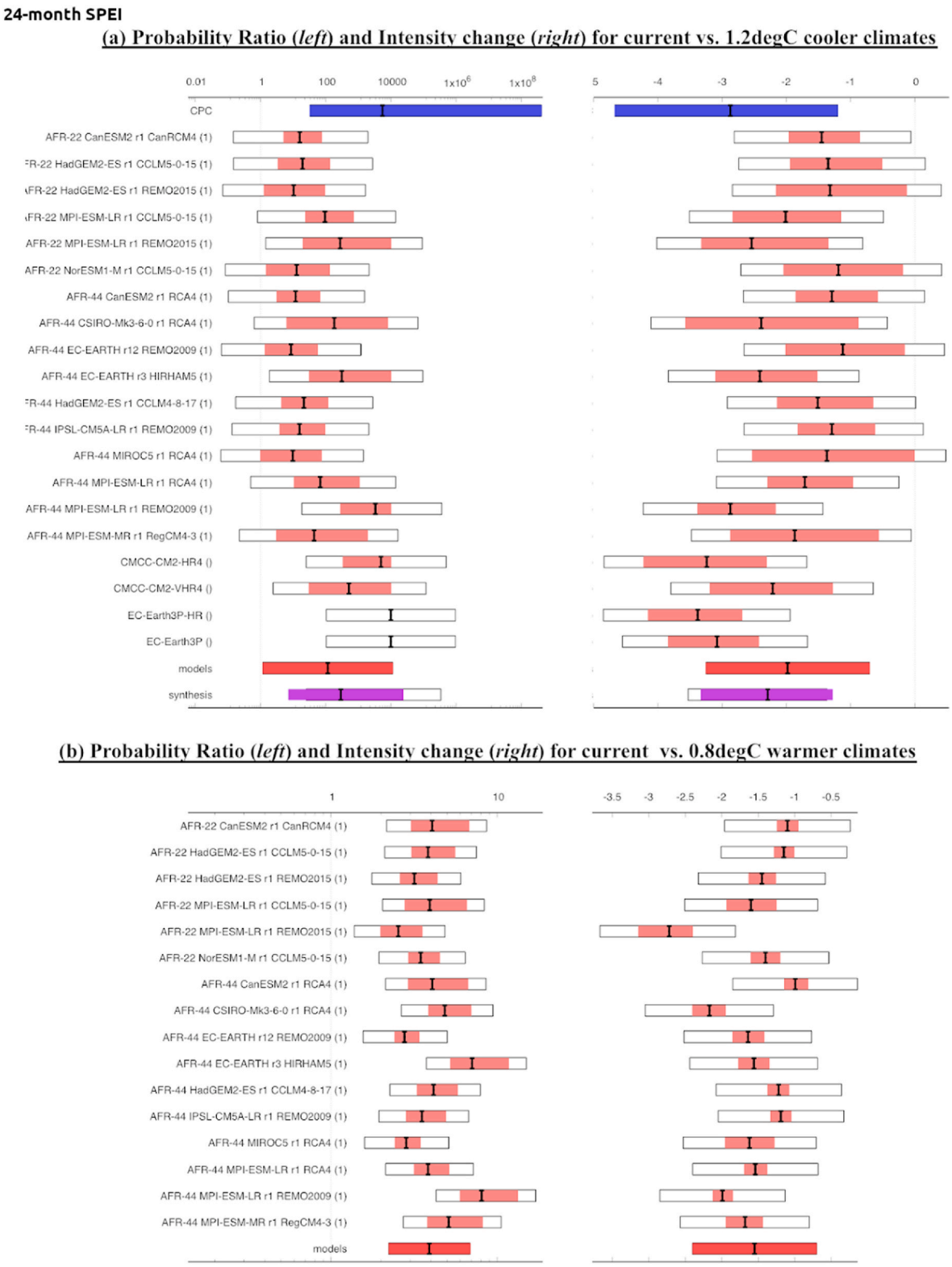


**Fig. 11.** (**a**) Synthesis of probability ratios (left) and intensity changes (in SPEI units; right) when comparing the return period and magnitudes of the 24-month SPEI over 2021–2022 for EA in the current climate and a 1.2 °C cooler climate. (**b**) Same as (**a**) in the current climate and a future 0.8 °C warmer climate.

management in the country. The NDMA provides drought early warning bulletins, develops drought management policies, and offers general planning of programmes. Through NDMA's strategic plan, the Kenyan government has taken an integrated approach to drought risk management in which NDMA coordinates drought interventions of the various government institutions. Other initiatives have also been taken by HoA countries to respond to the drought over the last few years. In Kenya, a flash drought appeal launched by the government and humanitarian organisations supported 1.7 million people between October 2021 and late 2022, and the Kenyan Red Cross activated an early action protocol in October 2022 to support at-risk farmers (IFRC, 2022).

In Somalia, the fragmented nature of drought management reflects a

**Table 2**
EM-DAT Drought events and associated impacts on populations (1900–2022).

| Country | Drought years | Number of events | Number of deaths | Number of people affected |
|---|---|---|---|---|
| Ethiopia | 1965, 1969, 1973, 1983, 1987, 1989, 1997, 1998, 1999, 2003, 2005, 2008, 2009, 2010, 2011, 2015, 2021, 2022 | 18 | 402,367 | 108,041,879 |
| Kenya | 1965, 1971, 1979, 1983, 1991, 1994, 1996, 1999, 2004, 2005, 2008, 2010, 2011, 2014, 2016, 2019, 2020 | 17 | 196 | 59,300,000 |
| Somalia | 1964, 1969, 1974, 1980, 1983, 1987, 1988, 1999, 2004, 2005, 2008, 2010, 2011, 2014, 2015, 2019, 2020 | 17 | 39,673 | 29,019,124 |

situation of chronic humanitarian needs and limited resources, reduced institutional presence and capacity in certain areas. A national drought plan was passed by the government in 2020 (UNCCD, 2020). The plan was complemented by a drought "Impact & Needs Assessment'' run in 2020 which notably studied cross-sectoral drought impacts and needs, and in turn informed the country's "Recovery and Resilience Framework" which sets pathways for resilience building at various levels (UNDP, 2020).

Ethiopia has a regional drought risk management mechanism in which every region has a disaster response fund (Oxfam, 2022). Lessons from the 2011 drought response led to the launch of a "Disaster Management and Food Security Agency'' in 2013 (GFDRR, 2013).

Kenya and Somalia are covered by the African Risk Capacity, a disaster risk insurance mechanism of the African Union that allows humanitarian organisations to match funds with existing insurance policies. In early 2023, Somalia received a payout of USD3.38 million from this fund (Start Network, 2023).

Generally, there is limited academic research about the achievements and challenges of all these policies and insurance schemes, and this will certainly warrant deeper investigation given the rise in humanitarian operations. Notably, questions about the applicability of current systems to multiple consecutive failed rainy seasons and the effectiveness of policies in alleviating impacts on food security and human health. Drought response plans in the three countries are currently significantly underfunded compared to the needs estimated by the humanitarian sector (see, Table 3; OCHA, 2023a; New Humanitarian, 2022). Further research is also required to understand whether government policies and humanitarian and development interventions have avoided potential impacts, and to what extent these systems are contributing to longer-term resilience or reliance.

#### 4.3.2. Household coping strategies

Exposed to recurring weather and climate extremes, households require coping strategies that are constructive rather than erosive, to help them endure and adapt to drought by finding viable alternatives to current socio-economic practices. Among the various categories of coping strategies (e.g., Quandt, 2021) diversification and long-term changes to livelihood have been considered highly constructive (Levine et al, nd; Prieto-Garcia et al., 2022; Taye et al., 2019; Yayeh Ayal et al., 2022). On the other hand, common coping activities among pastoralists are mobility and herd diversification (Lelamo et al., 2022), which can be erosive if a new livelihood is not secured in the new location, rendering people dependent on humanitarian assistance. This is the case for most displaced persons in Somalia (ACAPS, 2022). Erosive measures are often considered maladaptive as they entail strategies which bring adverse impact on humans or the environment, exacerbate risks, or are unsustainable in the long run (Ahmed et al., 2017). Further

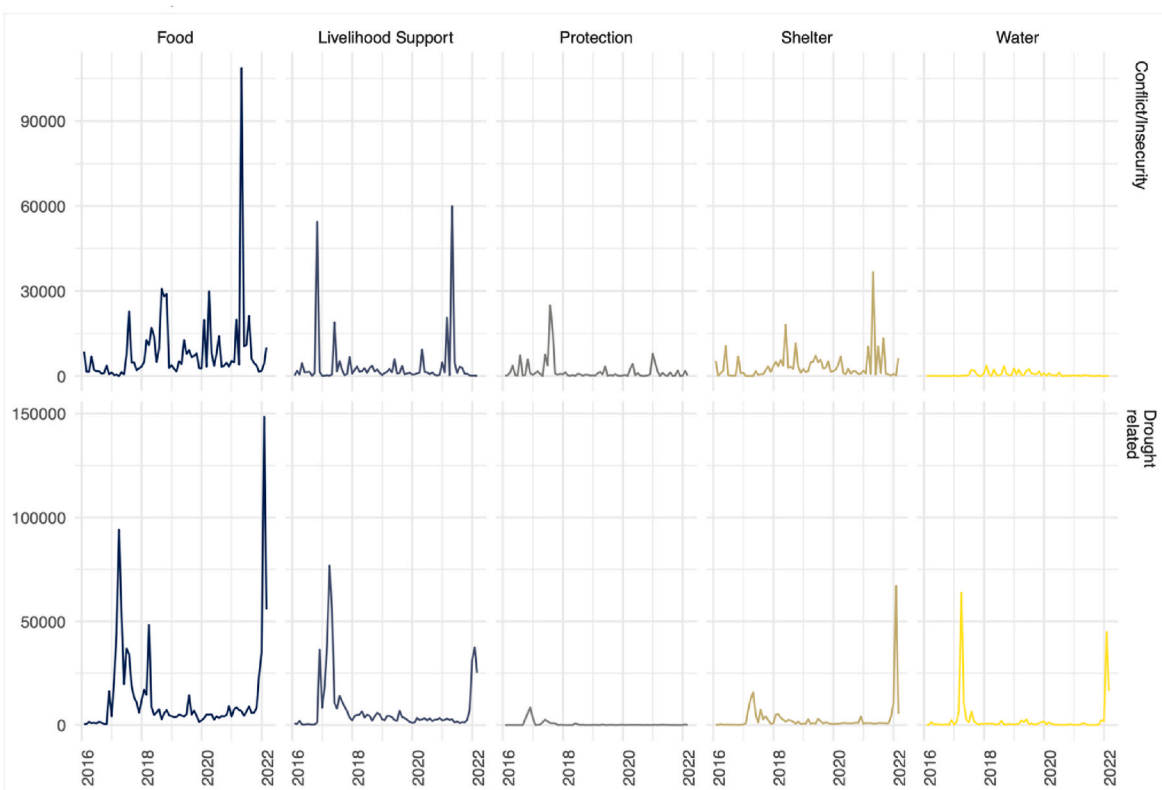


**Fig. 12.** Priority needs of drought and conflict affected IDPs in Somalia from Jan 2016 to Dec 2022. Data: UNHCR, 2023.

**Table 3**
Status of Drought/Humanitarian Response plans funding(OCHA, 2023a; financial tracking service).

| Country | Kenya | Ethiopia | Somalia |
|---|---|---|---|
| **Funded action Requirements** | USD 65.9 million<br>USD 451.8 million | USD 781.6 million<br>USD 3 994.8 million | USD 582.8 million<br>USD 2 599.2 million |
| **Summary of action clusters** | Education, Food security and livelihoods, Health, Nutrition, Protection, Water, sanitation, and hygiene | Camp Coordination and Camp Management, Education, Food security and livelihoods, Health, Logistics, Nutrition, Protection, Refugee Response, Shelter and NFIs, Water, sanitation, and hygiene | Agriculture, Camp Coordination and Camp Management, Camp Coordination and Camp Management, Education, Food, Health, Logistics, Nutrition, Protection, Protection, Shelter and NFIs, Water, sanitation, and hygiene |

examples include burning and selling charcoal, selling or slaughtering livestock, livestock off-take, children dropping out of school to support the household, and reliance on food assistance (Lwanga-Ntale and Owino, 2020; Quandt, 2021; Taye et al., 2019; Waaben Thulstrup et al., 2020). The latter is common among agropastoralists in Somalia (ACAPS, 2022; Lelamo et al., 2022).

Risk perception is fundamental to engaging in coping activities (Quandt, 2021). While experiences differ between pastoralists and agropastoralists, there is evidence that climate risk perception has improved over the past few decades (Abdullah and Mohamed, 2022; Abrham and Mekuyie, 2022; Bogale and Erena, 2022; Habte et al., 2022). With the erratic weather and the prolonged evolving and compounding state of crisis in the region, it is challenging to find adequate coping strategies, especially for marginalised groups with limited capacity. Barriers to undertaking coping strategies abound and include limited finances, expertise, risk information, government support, access to irrigation, shortage of land, labour, and finance; as well as conflict (Debela et al., 2019). The ability to translate one's risk perception into non-erosive action moreover depends on the economic, social, and cultural capital households can leverage. Beyond drought risk knowledge and information, undertaking coping activities notably requires financial viability and social connectedness (Abdullah and Mohamed, 2022; Lwanga-Ntale and Owino, 2020; Ndiritu, 2021; Quandt, 2021).

#### *4.3.3. Social protection*

Kenya and Ethiopia have strong social protection systems which are often regarded as flagship examples for the broader region. In Kenya, this includes the Hunger Safety Net Programme (HSNP), the Older Persons Cash Transfer (OPCT) programme, Cash Transfers for Orphans and Vulnerable Children (OVC), and Persons with Severe Disability Cash Transfer (PWSD-CT) programmes. HSNP, run by NDMA, aims to provide financial security to, and reduce hunger of, the most vulnerable Kenyans, especially in the Arid and Semi-Arid Lands (ASAL) of Northern Kenya (HSNP, 2023). As of June 2022, the HSNP's reach includes 149, 000 households (NDMA, 2022b) and four counties collectively reaching one million households across Kenya (FEWSNET, 2023). HSNP scales its support to vulnerable households up or down depending on the severity of droughts defined using the Vegetation Condition Index, with the system designed to include 75% more vulnerable households in affected areas (HSNP, 2023).

In 2005, Ethiopia launched Productive Safety Net Programme (PSNP), a multi-billion-dollar program that enhances food and economic security, while building resilience against crises. The PSNP provides cash payments to able-bodied members in exchange for labour contributions toward public works projects, and it provides direct payment for six months of the year to more vulnerable households. Relative to non-beneficiaries, PSNP recipients experienced 57 percent lower impacts of drought on food security (Scognamillo and Mastrorillo, 2022) and positive resilience outcomes at a household level (Abay et al., 2022). Notably, recipients were able to absorb drought shocks more quickly (less than two years) and were 48% less likely to face crop failure (Scognamillo and Mastrorillo, 2022). However, the ongoing conflict in Ethiopia's Tigray, Amhara and Afar regions have impacted the PSNPs timelines and reach (New Humanitarian, 2022).

In Somalia, social safety net programs are predominantly delivered via NGOs and local administrators with support from international partners. Approaches include both conditional and unconditional cash transfer programs as well public work programmes and school feeding programs. In 2019, the Government of Somalia, UNICEF and the World Bank jointly launched the Shock-Responsive Safety Net for Human Capital Project (SNHCP), known as *Baxnaano*. The project incorporates a short and long-term strategy that include unconditional cash transfers (20USD per month), enhancing social safety net delivery systems and institutional capacity building (WFP, 2021; World Bank, 2022). In 2020 the programme reached 1.2 million people across Somalia,

Based on historical events, the HSNP and the PSNP are critical components in mitigating what could be worse impacts of the ongoing drought. At the same time the drought severity and extent require support beyond these systems. This signals a need to further scale the systems geographic extent (especially in Kenya), while also underscoring the need for social protection and humanitarian systems to work hand-in-hand during emergencies.

## 5. Summary and conclusions

Evaluation of the role of human influence on the severity of drought induced by five consecutive failed rainfall seasons from 2020 until 2022 over a defined region in the Greater Horn of Africa was undertaken using multi-method multi-model event-attribution approaches. The analysis largely follows the standard World Weather Attribution protocol, supplemented with additional analysis of the role of the detrended Nino3.4 index in rainfall trends, and decomposition of the trend in Standardised Precipitation Evapotranspiration Index (SPEI) into contributions from precipitation and PET. Climate models and observational datasets were used to evaluate changes in 24-month (January 2021–December 2022) average rainfall, 24-month (January 2021–December 2022) Standardised Precipitation Evapotranspiration Index (SPEI), and seasonal average rainfall in both 2022 March-April-May and October-November-December seasons. The study also examined the existing vulnerability and exposure during the 2021–2022 drought to gain a broader understanding of the impacts.

Results show that in the climate of 2022, which has been warmed about 1.2 °C by human-induced greenhouse gas emissions, the 2021–2022 drought was exceptional due to climate change. The 24-month SPEI, combining the effects of precipitation changes and temperature-driven evapotranspiration, shows a strong increase in the likelihood of a drought of this severity, or equivalently, an increase in the intensity of a 1-in-20-year drought event. Findings also show a trend towards drying in the MAM and wettening over the OND. We do not find a trend in the 24-month precipitation. The years of the drought also saw consecutive La Niña conditions, known to be associated with below-average rainfall in the OND rains. In a future scenario with a 2 °C warmer world, drought conditions are still projected, though the changes are expected to be much smaller compared to the shifts observed from the past to the present. This may partly be due to the projected wetting trend in the region, particularly during OND, as indicated by models. Although these models are known to have significant biases in simulating East African climate, the wetting trends in OND could suggest potential shifts in planting seasons, with substantial implications for agriculture in the region.

The impacts of the 2021–2022 drought were (and still are) far-

reaching; touching on aspects such as health, food security, livelihoods, displacement, electricity infrastructure, security, and governance. Factors like disaster management and response functions, international aid, livelihood type, socio-economic status, state fragility, and the length of the drought played a key role in determining where and for whom impacts were greatest. Given the anthropogenically induced drying trend in rainfall, there are implications for both short-term drought management and long-term adaptation. A focus on reduction of vulnerability and exposure, approaches that are robust to both wet and dry extremes and increasing the capacity of people to cope with these types of events is needed to support short-term and long-term adaptation and resilience. However, questions remain whether soft or hard adaptation limits have been reached — while more and better designed drought response measures may help decrease poverty and increase resilience to shocks when they occur, certain crops, animals, and by extension livelihoods may become increasingly difficult to sustain in the changing climate.

## CRediT authorship contribution statement

**Joyce Kimutai:** Conceptualization, Formal analysis, Methodology, Writing – original draft. **Clair Barnes:** Formal analysis, Methodology. **Mariam Zachariah:** Writing – review & editing. **Sjoukje Y. Philip:** Writing – review & editing. **Sarah F. Kew:** Formal analysis. **Izidine Pinto:** Writing – review & editing. **Piotr Wolski:** Investigation. **Gerbrand Koren:** Writing – review & editing. **Gabriel Vecchi:** Resources. **Wenchang Yang:** Resources. **Sihan Li:** Visualization. **Maja Vahlberg:** Writing – review & editing. **Roop Singh:** Writing – review & editing. **Dorothy Heinrich:** Writing – review & editing. **Julie Arrighi:** Writing – review & editing. **Carolina Pereira Marghidan:** Writing – review & editing. **Lisa Thalheimer:** Writing – review & editing. **Cheikh Kane:** Writing – review & editing. **Emmanuel Raju:** Supervision, Writing – review & editing. **Friederike E.L. Otto:** Conceptualization, Supervision, Writing – review & editing.

## Declaration of competing interest

The authors declare that they have no known competing financial interests or personal relationships that could have appeared to influence the work reported in this paper.

## Acknowledgements

The authors acknowledge the support received from the European Union's Horizon 2020 research and innovation programme under XAIDA project, grant agreement No. 101003469.

JK, ER and FO acknowledge funding from the Danida Fellowship Centre (DFC), Ministry of Foreign Affairs of Denmark- Climate Change Attribution and Vulnerability in Kenya, DFC File No- 23-12-KU.

The authors acknowledgment to Karin who contributed to the discussions.

## Appendix A. Supplementary data

Supplementary data to this article can be found online at https://doi.org/10.1016/j.wace.2025.100745.

## Data availability

Almost all data is available via the KNMI Climate Explorer. Python notebooks used in the preparation and analysis of the observation and model data are available via GitHub.

## References

Abay, K.A., Abay, M.H., Berhane, G., Chamberlin, J., 2022. Social protection and resilience: the case of the productive safety net program in Ethiopia. Food Policy 112, 102367. https://doi.org/10.1016/J.FOODPOL.2022.102367.

Abdullah, M.Y., Mohamed, S.A., 2022. Perception of Climate Variability and its Impact by Smallholders in Pastoral Systems of Abudwak District, Galmudug State, Somalia. https://doi.org/10.21203/rs.3.rs-1243519/v1.

Abrham, T., Mekuyie, M., 2022. Effects of climate change on pastoral households in the Harshin District of the Somali Region, Ethiopia. Jàmbá : Journal of Disaster Risk Studies 14 (1), 2072–2845. https://doi.org/10.4102/JAMBA.V14I1.1202.

ACAPS, 2022. KEY FINDINGS CRISIS IMPACT OVERVIEW.

Ahmed, M., Uddin, I., Chowdhury, A., Subah Mohona, S., 2017. Access to credits and erosive or non-erosive coping strategies: an empirical analysis in Bangladesh. Eurasian Journal of Business and Economics 10 (19), 1–18. https://doi.org/10.17015/ejbe.2017.019.01.

Allen, R.G., Pereira, L.S., Raes, D., Smith, M., 1998. Crop Evapotranspiration-Guidelines for Computing Crop Water Requirements-FAO Irrigation and Drainage Paper 56.

Almorox, J., Quej, V.H., Martí, P., 2015. Global Performance Ranking of Temperature-Based Approaches for Evapotranspiration Estimation Considering Köppen Climate Classes. https://doi.org/10.1016/j.jhydrol.2015.06.057.

Amatya, D.M., Skaggs, R.W., Gregory, J.D., 1995. Comparison of methods for estimating REF-ET. J. Irrigat. Drain. Eng. 121 (6), 427–435. https://doi.org/10.1061/(ASCE)0733-9437(1995)121:6(427.

Amissah-Arthur, A., Jagtap, S., Rosenzweig, C., 2002. Spatio-temporal effects of El Niño events on rainfall and maize yield in Kenya. Int. J. Climatol. 22 (15), 1849–1860. https://doi.org/10.1002/JOC.858.

Arias, C., Lino, G., Sánchez, E., Nogués, S., Serrat, X., 2023. Drought impact on the morpho-physiological parameters of perennial rhizomatous grasses in the mediterranean environment. Agriculture (Switzerland) 13 (6), 1233. https://doi.org/10.3390/AGRICULTURE13061233/S1.

Asmall, T., Abrams, A., Röösli, M., Cissé, G., Carden, K., Dalvie, M.A., 2021. The adverse health effects associated with drought in Africa. Sci. Total Environ. 793, 148500. https://doi.org/10.1016/J.SCITOTENV.2021.148500.

Baier, W., Robertson, W.G., 1965. ESTIMATION OF LATENT EVAPORATION FROM SIMPLE WEATHER OBSERVATIONS, vol. 45, 442.

Beguería, S., Vicente-Serrano, S.M., Reig, F., Latorre, B., 2014. Standardized precipitation evapotranspiration index (SPEI) revisited: parameter fitting, evapotranspiration models, tools, datasets and drought monitoring. Int. J. Climatol. 34 (10), 3001–3023. https://doi.org/10.1002/joc.3887.

Bogale, G.A., Erena, Z.B., 2022. Drought vulnerability and impacts of climate change on livestock production and productivity in different agro-Ecological zones of Ethiopia. J. Appl. Anim. Res. 50 (1), 471–489. https://doi.org/10.1080/09712119.2022.2103563.

BOM, 2022. A wet spring: what is a "negative Indian Ocean Dipole" and why does it mean more rain for Australia's east? https://theconversation.com/a-wet-spring-what-is-a-negative-indian-ocean-dipole-and-why-does-it-mean-more-rain-for-australias-east-188167.

Buhaug, H., Benjaminsen, T.A., Gilmore, E.A., Hendrix, C.S., 2023. Climate-driven risks to peace over the 21st century. Climate Risk Management 39, 100471. https://doi.org/10.1016/J.CRM.2022.100471.

Chan, D., Vecchi, G.A., Yang, W., Huybers, P., 2021. Improved simulation of 19th-and 20th-century North Atlantic hurricane frequency after correcting historical sea surface temperatures. Sci. Adv. 7 (26), 6931–6956. https://doi.org/10.1126/SCIADV.ABG6931/SUPPL_FILE/ABG6931_SM.PDF.

Chen, M., Shi, W., Xie, P., Silva, V.B.S., Kousky, V.E., Higgins, R.W., Janowiak, J.E., 2008. Assessing objective techniques for gauge-based analyses of global daily precipitation. J. Geophys. Res. Atmos. 113 (4). https://doi.org/10.1029/2007JD009132.

Ciavarella, A., Cotterill, D., Stott, P., Kew, S., Philip, S., van Oldenborgh, G.J., Skålevåg, A., Lorenz, P., Robin, Y., Otto, F., Hauser, M., Seneviratne, S.I., Lehner, F., Zolina, O., 2021. Prolonged Siberian heat of 2020 almost impossible without human influence. Clim. Change 166 (1–2), 1–18. https://doi.org/10.1007/S10584-021-03052-W/TABLES/3.

Climate Hazards Center, 2023. Updated climate forecasts continue to suggest below-normal 2023 march-april-may rains likely in eastern horn of Africa | climate hazards center. https://blog.chc.ucsb.edu/?p=1263.

Dai, A., 2011. Characteristics and trends in various forms of the palmer drought severity index during 1900–2008. J. Geophys. Res. Atmos. 116 (D12), 12115. https://doi.org/10.1029/2010JD015541.

Dai, A., 2013. Increasing drought under global warming in observations and models. Nat. Clim. Change 3 (1), 52–58. https://doi.org/10.1038/NCLIMATE1633.

Debela, N., McNeil, D., Bridle, K., Mohammed, C., Debela, N., McNeil, D., Bridle, K., Mohammed, C., 2019. Adaptation to climate change in the pastoral and agropastoral systems of borana, south Ethiopia: options and barriers. Am. J. Clim. Change 8 (1), 40–60. https://doi.org/10.4236/AJCC.2019.81003.

Delworth, T.L., Rosati, A., Anderson, W., Adcroft, A.J., Balaji, V., Benson, R., Dixon, K., Griffies, S.M., Lee, H.C., Pacanowski, R.C., Vecchi, G.A., Wittenberg, A.T., Zeng, F., Zhang, R., 2012. Simulated climate and climate change in the GFDL CM2.5 high-resolution coupled climate model. J. Clim. 25 (8), 2755–2781. https://doi.org/10.1175/JCLI-D-11-00316.1.

Droogers, P., Allen, R.G., 2002. Estimating reference evapotranspiration under inaccurate data conditions. Irrigat. Drain. Syst. 16 (1), 33–45. https://doi.org/10.1023/A:1015508322413.

EM-DAT - The international disaster database. (n.d.). Retrieved October 31, 2023, from https://www.emdat.be/.

Eriksen, S., Schipper, E.L.F., Scoville-Simonds, M., Vincent, K., Adam, H.N., Brooks, N., Harding, B., Khatri, D., Lenaerts, L., Liverman, D., Mills-Novoa, M., Mosberg, M., Movik, S., Muok, B., Nightingale, A., Ojha, H., Sygna, L., Taylor, M., Vogel, C., West, J.J., 2021. Adaptation interventions and their effect on vulnerability in developing countries: help, hindrance or irrelevance? World Dev. 141, 105383. https://doi.org/10.1016/J.WORLDDEV.2020.105383.

FAO, 2022. The Threat of Starvation Looms in East Africa after Four Failed Rainy Seasons Situation May Worsen Due to Prospects of an Unprecedented Fifth Poor Season, 2022.

Feng, T., Su, T., Ji, F., Zhi, R., Han, Z., 2018. Temporal characteristics of actual evapotranspiration over China under global warming. J. Geophys. Res. Atmos. 123 (11), 5845–5858. https://doi.org/10.1029/2017JD028227.

FEWS NET, 2022. As deaths continue to accumulate despite assistance, Somalia is projected to face Famine in 2023 | FEWS NET. https://fews.net/east-africa/somalia/alert/december-2022.

FEWS NET, 2023. Death toll rises despite No official famine declaration in Somalia | FEWS NET. https://fews.net/death-toll-rises-despite-no-official-famine-declaration-somalia.

FEWSNET, 2023. Humanitarian food aid mitigating worse outcomes, though needs continue to outpace assistance levels | FEWS NET. https://fews.net/east-africa/kenya/food-security-outlook/february-2023.

Funk, C., 2020. Ethiopia, Somalia and Kenya face devastating drought. Nature 586 (7831), 645. https://doi.org/10.1038/D41586-020-02698-3.

Funk, C., Harrison, L., Shukla, S., Pomposi, C., Galu, G., Korecha, D., Husak, G., Magadzire, T., Davenport, F., Hillbruner, C., Eilerts, G., Zaitchik, B., Verdin, J., 2018. Examining the role of unusually warm Indo-Pacific sea-surface temperatures in recent African droughts. Q. J. R. Meteorol. Soc. 144 (June 2017), 360–383. https://doi.org/10.1002/qj.3266.

Funk, C., Nicholson, S.E., Landsfeld, M., Klotter, D., Peterson, P., Harrison, L., 2015a. The centennial trends greater horn of Africa precipitation dataset. Sci. Data 2 (1), 1–17. https://doi.org/10.1038/sdata.2015.50, 2(1).

Funk, C., Peterson, P., Landsfeld, M., Pedreros, D., Verdin, J., Shukla, S., Husak, G., Rowland, J., Harrison, L., Hoell, A., Michaelsen, J., 2015b. The climate hazards infrared precipitation with stations - a new environmental record for monitoring extremes. Sci. Data 2, 1–21. https://doi.org/10.1038/sdata.2015.66.

Funk, C., Shukla, S., Thiaw, W.M., Rowland, J., Hoell, A., Mcnally, A., Husak, G., Novella, N., Budde, M., Peters-Lidard, C., Adoum, A., Galu, G., Korecha, D., Magadzire, T., Rodriguez, M., Robjhon, M., Bekele, E., Arsenault, K., Peterson, P., et al., 2019. Recognizing the famine early warning systems Network: over 30 Years of drought early warning science advances and partnerships promoting global food security. Bull. Am. Meteorol. Soc. 100 (6), 1011–1027. https://doi.org/10.1175/BAMS-D-17-0233.1.

Getie, E.M., 2020. Poverty of energy and its impact on living standards in Ethiopia. Journal of Electrical and Computer Engineering 2020. https://doi.org/10.1155/2020/7502583.

GFDRR, 2013. COUNTRY PROGRAM UPDATE MAY 2013 KEY PRIORITIES RELATED TO DRM IN THE COUNTRY.

*globalwarmingindex.org – Tracking progress to a safe climate*. (n.d.). Retrieved October 31, 2023, from https://www.globalwarmingindex.org/.

Graham, A., Aubry, S., Künnemann, R., Monsalve Suárez, S., Monsalve Suárez -Fian, S., 2009. The role of the EU in land grabbing in Africa-CSO "advancing african agriculture" (AAA): the impact of europe's policies and practices on african agriculture and food security. http://www.oilwatchafrica.org/sites/all/files/enicongoreport.pdf.

Greve, P., Roderick, M., et al., 2019. The aridity index under global warming. & 2019, undefined Iopscience.Iop.OrgP Greve. https://doi.org/10.1088/1748-9326/ab5046. ML Roderick, AM Ukkola, Y WadaEnvironmental Research Letters, 2019•iopscience. *Iop.Org*.

Haarsma, R.J., Roberts, M.J., Vidale, P.L., Catherine, A., Bellucci, A., Bao, Q., Chang, P., Corti, S., Fučkar, N.S., Guemas, V., Von Hardenberg, J., Hazeleger, W., Kodama, C., Koenigk, T., Leung, L.R., Lu, J., Luo, J.J., Mao, J., Mizielinski, M.S., et al., 2016. High resolution model Intercomparison project (HighResMIP v1.0) for CMIP6. Geosci. Model Dev. (GMD) 9 (11), 4185–4208. https://doi.org/10.5194/GMD-9-4185-2016.

Habte, M., Eshetu, M., Maryo, M., Andualem, D., Legesse, A., 2022. Effects of climate variability on livestock productivity and pastoralists perception: the case of drought resilience in Southeastern Ethiopia. Veterinary and Animal Science 16, 100240. https://doi.org/10.1016/J.VAS.2022.100240.

Haile, G.G., Tang, Q., Hosseini-Moghari, S.M., Liu, X., Gebremicael, T.G., Leng, G., Kebede, A., Xu, X., Yun, X., 2020. Projected impacts of climate change on drought patterns over East Africa. Earths Future 8 (7), e2020EF001502. https://doi.org/10.1029/2020EF001502.

Hansen, J., Ruedy, R., Sato, M., Lo, K., 2010. Global surface temperature change. Rev. Geophys. 48 (4). https://doi.org/10.1029/2010RG000345.

Hargreaves, G.H., Samani, Z.A., 1985. Reference crop evapotranspiration from temperature. Appl. Eng. Agric. 1 (2), 96–99. https://doi.org/10.13031/2013.26773.

Hersbach, H., Bell, B., Berrisford, P., Hirahara, S., Horányi, A., Muñoz-Sabater, J., Nicolas, J., Peubey, C., Radu, R., Schepers, D., Simmons, A., Soci, C., Abdalla, S., Abellan, X., Balsamo, G., Bechtold, P., Biavati, G., Bidlot, J., Bonavita, M., et al., 2020. The ERA5 global reanalysis. Q. J. R. Meteorol. Soc. 146 (730), 1999–2049. https://doi.org/10.1002/qj.3803.

Hill, R.V., Porter, C., 2017. Vulnerability to drought and food price shocks: evidence from Ethiopia. World Dev. 96, 65–77. https://doi.org/10.1016/J.WORLDDEV.2017.02.025.

Hoell, A., Funk, C., 2014. Indo-Pacific sea surface temperature influences on failed consecutive rainy seasons over eastern Africa. Clim. Dyn. 43 (5–6), 1645–1660. https://doi.org/10.1007/s00382-013-1991-6.

Homewood, K., Kristjanson, P., Trench, P.C., 2009. Changing Land Use, Livelihoods and Wildlife Conservation in Maasailand, pp. 1–42. https://doi.org/10.1007/978-0-387-87492-0_1.

HSNP, 2023. About HSNP. https://www.hsnp.or.ke/index.php/as/objectives.

IFRC, 2022. Kenya: drought - early action protocol summary (EAP2022KE02) - Kenya | ReliefWeb. https://reliefweb.int/report/kenya/kenya-drought-early-action-protocol-summary-eap2022ke02.

IPCC, 2012. IPCC SREX. Ipcc, vol. 594. https://www.ipcc.ch/pdf/special-reports/srex/SREX_Full_Report.pdf/5Cnpapers2://publication/uuid/41AD43FB-2529-4ACD-AD33-4C2D0AB4A0F3/5Cn.

Jensen, M.E., Burman, R.D., Allen, R.G., 1990. Evapotranspiration and irrigation water requirements. ASCE manuals and reports on engineering practice No. 70. ASCE Manuals and Reports on Engineering Practice No. 70 360. https://books.google.com/books/about/Evapotranspiration_and_Irrigation_Water.html?id=Z22jnQEACAAJ.

Jung, M., Reichstein, M., Ciais, P., Seneviratne, S.I., Sheffield, J., Goulden, M.L., Bonan, G., Cescatti, A., Chen, J., de Jeu, R., Johannes Dolman, A., Eugster, W., Gerten, D., Gianelle, D., Gobron, N., Heinke, J., Kimball, J., Law, B.E., Montagnani, L., et al., 2010. Recent Decline in the Global Land Evapotranspiration Trend Due to Limited Moisture Supply. https://doi.org/10.1038/nature09396.

Kenya Govt., 2023. EXECUTIVE OFFICE OF THE PRESIDENT. PRESS RELEASE.

Kew, S.F., Philip, S.Y., Hauser, M., Hobbins, M., Wanders, N., Jan Van Oldenborgh, G., Van Der Wiel, K., Veldkamp, T.I.E., Kimutai, J., Funk, C., Otto, F.E.L., 2021. Impact of precipitation and increasing temperatures on drought trends in eastern Africa. Earth System Dynamics 12 (1), 17–35. https://doi.org/10.5194/ESD-12-17-2021.

Kimutai, J., New, M., Wolski, P., Otto, F., 2022. Attribution of the human influence on heavy rainfall associated with flooding events during the 2012, 2016, and 2018 March-April-May seasons in Kenya. Weather Clim. Extrem. 38, 100529.

KMD, 2023. (20) Kenya Met Department KE on X: " MAM (Mar-Apr-May) is an essential rainfall season for KE's agriculture in Western, Rift Valley & Central. This weekend: light-moderate in some areas with an increase in intensity from Monday = onset of the long rainy season Stay. updated at. https://twitter.com/MeteoKenya/status/1634286810741329942.

Koubi, V., 2019. Climate Change and Conflict, vol. 22, pp. 343–360. https://doi.org/10.1146/ANNUREV-POLISCI-050317-070830.

Krieger, T., Panke, D., Pregernig, M., 2020. Climate Change, Conflicts and Migration. Bristol University Press. https://bristoluniversitypressdigital.com/display/book/9781529202175/ch004.xml.

Lelamo, L.L., Shenkut, B.T., Abdilahi, A.H., 2022. Drought characteristics and pastoralists' response strategies in Korahey zone, Somali regional state, Eastern Ethiopia. Scientific African 16, e01254. https://doi.org/10.1016/J.SCIAF.2022.E01254.

Lenssen, N.J.L., Schmidt, G.A., Hansen, J.E., Menne, M.J., Persin, A., Ruedy, R., Zyss, D., 2019. Improvements in the GISTEMP uncertainty model. J. Geophys. Res. Atmos. 124 (12), 6307–6326. https://doi.org/10.1029/2018JD029522.

Levine, S., Humphrey, A., Weingärtner, L., & Abdi, M. (n.d.). UNDERSTANDING THE ROLE OF ANTICIPATORY ACTION IN SOMALIA. Retrieved October 31, 2023, from www.anticipation-hub.org.

Li, G., Zhang, F., Jing, Y., Liu, Y., 2017. Response of Evapotranspiration to Changes in Land Use and Land Cover and Climate in China during 2001–2013. Environment, G. S.-S. of the T., & 2017, undefined. Elsevier. https://www.sciencedirect.com/science/article/pii/S0048969717309178?casa_token=2lYuqzbe8pkAAAAA:eTisxoq89kVqVI2mneQvHoKDi79PLIhHNV0V83Cy19WC-jjFxLddZXozSYQGQv9I8n2e2QzEdQir.

Li, S., Kang, S., Zhang, L., Zhang, J., Du, T., 2016. Evaluation of Six Potential Evapotranspiration Models for Estimating Crop Potential and Actual Evapotranspiration in Arid Regions. Hydrology, L. T.-J. of, & 2016, undefined. Elsevier. https://www.sciencedirect.com/science/article/pii/S0022169416306667?casa_token=gE2NAsHbsGgAAAAA:BpibITPolh7NAeU9FMacnYetuAZ-dhnoyZ2XEHMmoYJiEmb15y1gzqHU41EiADcmZx3vqUfktndy.

Liebmann, B., Hoerling, M.P., Funk, C., Bladé, I., Dole, R.M., Allured, D., Quan, X., Pegion, P., Eischeid, J.K., 2014. Understanding recent eastern Horn of Africa rainfall variability and change. J. Clim. 27 (23), 8630–8645. https://doi.org/10.1175/JCLI-D-13-00714.1.

Lott, F.C., Christidis, N., Stott, P.A., 2013. Can the 2011 East African drought be attributed to human-induced climate change? Geophys. Res. Lett. 40 (6), 1177–1181. https://doi.org/10.1002/grl.50235.

Lu, J., Sun, G., McNulty, S.G., Amatya, D.M., 2005. A comparison of six potential evapotranspiration methods for regional use in the southeastern United States1. JAWRA Journal of the American Water Resources Association 41 (3), 621–633. https://doi.org/10.1111/J.1752-1688.2005.TB03759.X.

Lujano, A., Sanchez-Delgado, M., 2023. Improvement of hargreaves–samani reference evapotranspiration estimates in the Peruvian altiplano. Water, E. L.-, & 2023, undefined. https://www.mdpi.com/2073-4441/15/7/1410.

Lwanga-Ntale, C., Owino, B.O., 2020. Understanding vulnerability and resilience in Somalia. Jàmbá : Journal of Disaster Risk Studies 12 (1), 1–9. https://doi.org/10.4102/JAMBA.V12I1.856.

Marthews, T.R., Otto, F.E.L., Mitchell, D., Dadson, S.J., Jones, R.G., 2015. The 2014 drought in the horn of Africa: attribution of meteorological drivers. Bull. Am. Meteorol. Soc. 96 (12), S83–S88. https://doi.org/10.1175/BAMS-D-15-00115.1.

Mason, J.B., White, J.M., Heron, L., Carter, J., Wilkinson, C., Spiegel, P., 2012. Child acute malnutrition and mortality in populations affected by displacement in the horn of Africa, 1997–2009. Int. J. Environ. Res. Publ. Health 9 (3), 791. https://doi.org/10.3390/IJERPH9030791.

Meier, P., Bond, D., Bond, J., 2007. Environmental influences on pastoral conflict in the Horn of Africa. Polit. Geogr. 26 (6), 716–735. https://doi.org/10.1016/J.POLGEO.2007.06.001.
MPI, 2023. Article: amid Record Drought and Food Insecurity. migrationpolicy.org. https://www.migrationpolicy.org/article/east-africa-drought-food-insecurity-refugees.
Mutai, C., Climate, M. W.-J. of, & 2000, undefined. (n.d.). East African rainfall and the tropical circulation/convection on intraseasonal to interannual timescales. Journals. Ametsoc.OrgCC Mutai, MN WardJournal of Climate, 2000•journals.Ametsoc.Org. Retrieved October 31, 2023, from https://journals.ametsoc.org/view/journals/clim/13/22/1520-0442_2000_013_3915_earatt_2.0.co_2.xml?tab_body=pdf.
Ndiritu, S.W., 2021. Drought responses and adaptation strategies to climate change by pastoralists in the semi-arid area, Laikipia County, Kenya. Mitig. Adapt. Strategies Glob. Change 26 (3), 1–18. https://doi.org/10.1007/S11027-021-09949-2/TABLES/4.
NDMA, 2022a. Ndma - KnowledgeWeb. http://knowledgeweb.ndma.go.ke/Public/Resources/Default.aspx?ID=7&_gl=1*18c5ev9*_ga*MzU5NTgwNjgxLjE2OTg2Njc0Njc.*_ga_RVYWZRJTGS*MTY5ODY2NzQ2Ni4xLjEuMTY5ODY2NzU5MS4wLjAuMA.
NDMA, 2022b. NDMA Disburses Ksh1.1 Billion for Drought Affected Families - Kenya. ReliefWeb. https://reliefweb.int/report/kenya/ndma-disburses-ksh11-billion-drought-affected-families.
New Humanitarian, 2022. The New Humanitarian | Ethiopia's worsening drought sees hunger numbers soar. https://www.thenewhumanitarian.org/news-feature/2022/08/17/drought-Ethiopia-hunger-pastoralism-climate-change.
Nguvava, M., Abiodun, B.J., Otieno, F., 2019. Projecting drought characteristics over East African basins at specific global warming levels. Atmos. Res. 228, 41–54. https://doi.org/10.1016/J.ATMOSRES.2019.05.008.
Nicholson, S.E., 2016. An analysis of recent rainfall conditions in eastern Africa. Int. J. Climatol. 36 (1), 526–532. https://doi.org/10.1002/joc.4358.
Nicholson, S.E., 2017. Climate and climatic variability of rainfall over eastern Africa. Rev. Geophys. 55 (3), 590–635. https://doi.org/10.1002/2016RG000544.
Nikulin, G., Jones, C., Giorgi, F., et al., 2012. Precipitation climatology in an ensemble of CORDEX-Africa regional climate simulations. of, & 2012, undefined Journals. Ametsoc. OrgG Nikulin, C Jones, F Giorgi, G Asrar, M Büchner, R Cerezo-Mota, OB Christensen, M DéquéJournal of Climate, 2012•journals.Ametsoc.Org. https://journals.ametsoc.org/view/journals/clim/25/18/jcli-d-11-00375.1.xml?tab_body=fulltext-display.
Nikulin, G., Lennard, C., et al., 2018. The effects of 1.5 and 2 degrees of global warming on Africa in the CORDEX ensemble. Iopscience.Iop.Org. A. D.-E., & 2018, undefined. https://iopscience.iop.org/article/10.1088/1748-9326/aab1b1/meta.
Njiru, C.W., Letema, S.C., 2018. Energy poverty and its implication on standard of living in kirinyaga, Kenya. J. Energy 2018, 1–12. https://doi.org/10.1155/2018/3196567.
OCHA, 2023a. Home | financial tracking service. https://fts.unocha.org/home/2023/donors/view.
OCHA, 2023b. Kenya 2022 Drought Response in Review - Kenya. ReliefWeb. https://reliefweb.int/report/kenya/kenya-2022-drought-response-review.
OCHA, 2023c. Somalia: Drought - 2015-2023. ReliefWeb. https://reliefweb.int/disaster/dr-2015-000134-som.
OCHA, 2023d. WFP Kenya Country Brief, February 2023 - Kenya. ReliefWeb. https://reliefweb.int/report/kenya/wfp-kenya-country-brief-february-2023.
Ogallo, L.A., 1993. Validity of the ENSO-related impacts in eastern and southern Africa. http://erepository.uonbi.ac.ke/handle/11295/48694.
Ogallo, L.J., 1988. Relationships between seasonal rainfall in East Africa and the southern oscillation. J. Climatol. 8 (1), 31–43. https://doi.org/10.1002/JOC.3370080104.
OHCHR, 2020. Kenya's informal settlements need safe water to survive COVID-19 | OHCHR. https://www.ohchr.org/en/stories/2020/04/kenyas-informal-settlements-need-safe-water-survive-covid-19.
Omolo, N., Mafongoya, P.L., 2019. Gender, social capital and adaptive capacity to climate variability: a case of pastoralists in arid and semi-arid regions in Kenya. International Journal of Climate Change Strategies and Management 11 (5), 744–758. https://doi.org/10.1108/IJCCSM-01-2018-0009/FULL/PDF.
Otto, F.E.L., Raju, E., 2023. Harbingers of decades of unnatural disasters. Communications Earth & Environment 4 (1), 1–7. https://doi.org/10.1038/s43247-023-00943-x, 4(1).
Our World in Data, 2022a. Energy. Our World in Data, vol. 9, pp. 28–49. https://doi.org/10.1016/j.esr.2015.11.003.
Our World in Data, 2022b. Energy. Our World in Data, vol. 9, pp. 28–49. https://doi.org/10.1016/j.esr.2015.11.003.
Owain, E.L., Maslin, M.A., 2018. Assessing the relative contribution of economic, political and environmental factors on past conflict and the displacement of people in East Africa, 2018 Palgrave Communications 4 (1), 1–9. https://doi.org/10.1057/s41599-018-0096-6, 4(1).
Oxfam, 2022. Dangerous Delay 2: the Cost of Inaction. Oxfam International. https://www.oxfam.org/en/research/dangerous-delay-2-cost-inaction.
Palmer, P.I., Wainwright, C.M., Dong, B., Maidment, R.I., Wheeler, K.G., Gedney, N., Hickman, J.E., Madani, N., Folwell, S.S., Abdo, G., Allan, R.P., Black, E.C.L., Feng, L., Gudoshava, M., Haines, K., Huntingford, C., Kilavi, M., Lunt, M.F., Shaaban, A., Turner, A.G., 2023. Drivers and impacts of Eastern African rainfall variability. Nat. Rev. Earth Environ. 4 (4), 254–270. https://doi.org/10.1038/s43017-023-00397-x, 4(4).
Pape, U.J., Wollburg, P.R., 2019. Impact of drought on poverty in Somalia. https://papers.ssrn.com/abstract=3313863.
Paul, M., 2022. Drought in the Horn of Africa: more than 18.5 million in Ethiopia, Kenya, Somalia and Djibouti face humanitarian crisis. https://www.downtoearth.org.in/news/africa/drought-in-the-horn-of-africa-more-than-18-5-million-in-ethiopia-kenya-somalia-and-djibouti-face-humanitarian-crisis-83569.
Philip, S., Kew, S., van Oldenborgh, G.J., Otto, F., Vautard, R., van der Wiel, K., King, A., Lott, F., Arrighi, J., Singh, R., van Aalst, M., 2020. A protocol for probabilistic extreme event attribution analyses. Advances in Statistical Climatology, Meteorology and Oceanography 6 (2), 177–203. https://doi.org/10.5194/ascmo-6-177-2020.
Prieto-Garcia, J., 2022. Climate change in the horn of Africa drylands: domestification of Yeheb as a climate-smart agricultural mitigation strategy to protect the regional food chain. https://www.researchgate.net/profile/Muna-Ismail-2/publication/364651471_Climate_Change_in_Horn_of_Africa_Drylands_Domestication_of_Yeheb_as_a_Climate-Smart_Agricultural_Mitigation_Strategy_to_Protect_the_Regional_Food_Chain/links/635559b712cbac6a3eeb606d/Climate-Change-in-Horn-of-Africa-Drylands-Domestication-of-Yeheb-as-a-Climate-Smart-Agricultural-Mitigation-Strategy-to-Protect-the-Regional-Food-Chain.pdf.
Quandt, A., 2021. Coping with drought: narratives from smallholder farmers in semi-arid Kenya. Int. J. Disaster Risk Reduct. 57, 102168. https://doi.org/10.1016/J.IJDRR.2021.102168.
Raju, E., Boyd, E., Otto, F., 2022. Stop blaming the climate for disasters, 2022 Communications Earth & Environment 3 (1), 1–2. https://doi.org/10.1038/s43247-021-00332-2, 3(1).
Rayner, N.A., Parker, D.E., Horton, E.B., Folland, C.K., Alexander, L.V., Rowell, D.P., Kent, E.C., Kaplan, A., 2003. Global analyses of sea surface temperature, sea ice, and night marine air temperature since the late nineteenth century. J. Geophys. Res. Atmos. 108 (D14). https://doi.org/10.1029/2002JD002670.
Rowell, D.P., Senior, C.A., Vellinga, M., Graham, R.J., 2016. Can climate projection uncertainty be constrained over Africa using metrics of contemporary performance? Clim. Change 134 (4), 621–633. https://doi.org/10.1007/s10584-015-1554-4.
Rutten, M.M.E.M., 1992. Selling Wealth to Buy Poverty: the Process of the Individualization of Landownership Among the Maasai Pastoralists of Kajiado District, Kenya, 1890-1990. Breitenbach. https://hdl.handle.net/1887/9046.
Schapper, A., Unrau, C., Killoh, S., 2020. Social mobilization against large hydroelectric dams: a comparison of Ethiopia, Brazil, and Panama. Sustain. Dev. 28 (2), 413–423. https://doi.org/10.1002/SD.1995.
Scheff, J., Frierson, D.M.W., 2014. Scaling potential evapotranspiration with greenhouse warming. J. Clim. 27 (4), 1539–1558. https://doi.org/10.1175/JCLI-D-13-00233.1.
Schumacher, D.L., Keune, J., Dirmeyer, P., Miralles, D.G., 2022. Drought self-propagation in drylands due to land–atmosphere feedbacks. Nat. Geosci. 15 (4), 262–268. https://doi.org/10.1038/s41561-022-00912-7, 2022 15:4.
Scognamillo, A., Mastrorillo, M., 2022. Food and agriculture organization of the united nations rome, 2022. https://doi.org/10.4060/cc0824en.
Sheffield, J., Wood, E.F., Roderick, M.L., 2012. Little change in global drought over the past 60 years. https://doi.org/10.1038/nature11575.
Shepherd, A., Mitchell, T., Jones, L., Scott, L., 2015. The geography of poverty, disasters and climate extremes in 2030. https://odi.org/en/publications/the-geography-of-poverty-disasters-and-climate-extremes-in-2030/.
Sherwood, A., 2013. Community adaptation to climate change: exploring drought and poverty traps in Gituamba location, Kenya. J. Nat. Resour. Policy Res. 5 (2–3), 147–161. https://doi.org/10.1080/19390459.2013.811857.
Start Network, 2023. Start Network | A new era of humanitarian action. https://startnetwork.org/.
Tabari, H., Aghajanloo, M.-B., 2012. Temporal pattern of aridity index in Iran with considering precipitation and evapotranspiration trends. INTERNATIONAL JOURNAL OF CLIMATOLOGY Int. J. Climatol. https://doi.org/10.1002/joc.3432.
Tache, B., 2013. Rangeland enclosures in Southern Oromia, Ethiopia: an innovative response or the erosion of common property resources? Pastoralism and Development in Africa: Dynamic Change at the Margins 37–46. https://doi.org/10.4324/9780203105979.
Taye, M., Alulu, V., Gobu, W., Jensen, N., 2019. Livestock Insurance Payouts and Coping Strategies of Pastoralists during Drought.
Taylor, K.E., Stouffer, R.J., Meehl, G.A., 2012. An overview of CMIP5 and the experiment design. Bull. Am. Meteorol. Soc. 93 (4), 485–498. https://doi.org/10.1175/BAMS-D-11-00094.1.
Thalheimer, L., 2023. Compounding risks and increased vulnerabilities: climate change, conflict, and mobility in East Africa. Environmental Migration in the Face of Emerging Risks 137–153. https://doi.org/10.1007/978-3-031-29529-4_8/COVER.
Thalheimer, L., Otto, F., Abele, S., 2021a. Deciphering impacts and human responses to a changing climate in East Africa. Frontiers in Climate 3, 692114. https://doi.org/10.3389/FCLIM.2021.692114/BIBTEX.
Thalheimer, L., Webersik, C., 2021. Compound Vulnerabilities Exacerbate Systemic Risks of Food Security in Somalia. https://doi.org/10.21203/rs.3.rs-893022/v1.
Thalheimer, L., Webersik, C., Gaupp, F., 2021b. Compound Vulnerabilities Exacerbate Systemic Risks of Food Security in Somalia. https://doi.org/10.21203/rs.3.rs-893022/v1.
Thomas, K., Hardy, R.D., Lazrus, H., Mendez, M., Orlove, B., Rivera-Collazo, I., Roberts, J.T., Rockman, M., Warner, B.P., Winthrop, R., 2019. Explaining differential vulnerability to climate change: a social science review. Wiley Interdisciplinary Reviews: Clim. Change 10 (2). https://doi.org/10.1002/WCC.565.
Thornthwaite, C., 1948. An approach toward a rational classification of climate. JSTORCW ThornthwaiteGeographical Review, 1948•JSTOR. https://www.jstor.org/stable/210739?casa_token=Tb7kr8a_XxMAAAAA:VfQGiYDpMSSJ0gyuEbIWN_CHfPWbmaQ_JebgW2cvIV4p_lzAFgj2SEHqPYY87GGAXHXm4P8wWiQxY21o_lMB8hRPgVjmLhhbhyNhkc2-LrjTU1JcyzbJFw.
Trajkovic, S., 2007. Hargreaves versus penman-monteith under humid conditions. J. Irrigat. Drain. Eng. 133 (1), 38–42. https://doi.org/10.1061/(ASCE)0733-9437(2007)133:1(38.

Trajkovic, S., Gocic, M., Pongracz, R., Bartholy, J., Milanovic, M., 2020. Assessment of reference evapotranspiration by regionally calibrated temperature-based equations. KSCE J. Civ. Eng. 24 (3), 1020–1027. https://doi.org/10.1007/s12205-020-1698-2.

Tura, H.A., 2018. Land rights and land grabbing in Oromia, Ethiopia. Land Use Policy 70, 247–255. https://doi.org/10.1016/J.LANDUSEPOL.2017.10.024.

Uhe, P., Philip, S., Kew, S., Shah, K., Kimutai, J., Mwangi, E., van Oldenborgh, G.J., Singh, R., Arrighi, J., Jjemba, E., Cullen, H., Otto, F., 2018. Attributing drivers of the 2016 Kenyan drought. Int. J. Climatol. 38, e554–e568. https://doi.org/10.1002/joc.5389.

UNCCD, 2020. National drought plan and resilience framework for Somalia - climate change laws of the world. https://climate-laws.org/document/national-drought-plan-and-resilience-framework-for-somalia_cf96.

UNDP, 2020. Drought Impact and Needs Assessment and Recovery and Resilience Framework. United Nations Development Programme. https://www.undp.org/somalia/drought-impact-and-needs-assessment-and-recovery-and-resilience-framework.

UNDP, 2022. Briefing note for countries on the 2023 multidimensional poverty index Ethiopia what is the global multidimensional poverty index? Structure of the global multidimensional poverty index multidimensional poverty index for Angola. https://hdr.undp.org/mpi-2023-faqs.

UNFPA, 2022. Kenya: severe drought fuels malnutrition, reduces hospital-delivery births in Turkana County | UN News. https://news.un.org/en/story/2022/12/1132047.

UNHCR, 2023a. As the Horn of Africa drought enters a sixth failed rainy season, UNHCR calls for urgent assistance | UNHCR. https://www.unhcr.org/news/horn-africa-drought-enters-sixth-failed-rainy-season-unhcr-calls-urgent-assistance.

UNHCR, 2023b. Somalia: internal displacements. https://unhcr.github.io/dataviz-somalia-prmn/index.html#reason=&month=&need=&pregion=&pdistrictmap=&cregion=&cdistrictmap=&year=2021.

UNHCR, 2023c. The Horn of Africa Drought Situation Appeal (January - December 2023) - Ethiopia. ReliefWeb. https://reliefweb.int/report/ethiopia/horn-africa-drought-situation-appeal-january-december-2023.

UNHCR, 2023d. The Horn of Africa Drought Situation Appeal (January - December 2023) - Ethiopia. ReliefWeb. https://reliefweb.int/report/ethiopia/horn-africa-drought-situation-appeal-january-december-2023.

Van Der Schrier, G., Jones, P.D., Briffa, K.R., 2011. The sensitivity of the PDSI to the Thornthwaite and Penman-Monteith parameterizations for potential evapotranspiration. J. Geophys. Res. Atmos. 116 (D3). https://doi.org/10.1029/2010JD015001.

Van Oldenborgh, G.J., Hendon, H., Stockdale, T., L'Heureux, M., Coughlan De Perez, E., Singh, R., Van Aalst, M., 2021. Defining El Niño indices in a warming climate. Environ. Res. Lett. 16 (4), 044003. https://doi.org/10.1088/1748-9326/ABE9ED.

van Oldenborgh, G.J., van der Wiel, K., Kew, S., Philip, S., Otto, F., Vautard, R., King, A., Lott, F., Arrighi, J., Singh, R., van Aalst, M., 2021. Pathways and pitfalls in extreme event attribution. Clim. Change 166 (1–2), 1–27. https://doi.org/10.1007/S10584-021-03071-7/FIGURES/3.

Van Oldenborgh, G.J., Wehner, M.F., Vautard, R., Otto, F.E.L., Seneviratne, S.I., Stott, P.A., Hegerl, G.C., Philip, S.Y., Kew, S.F., 2022. Attributing and projecting heatwaves is hard: we can do better. Earths Future 10 (6), e2021EF002271. https://doi.org/10.1029/2021EF002271.

Vecchi, G.A., Delworth, T., Gudgel, R., Kapnick, S., Rosati, A., Wittenberg, A.T., Zeng, F., Anderson, W., Balaji, V., Dixon, K., Jia, L., Kim, H.S., Krishnamurthy, L., Msadek, R., Stern, W.F., Underwood, S.D., Villarini, G., Yang, X., Zhang, S., 2014. On the seasonal forecasting of regional tropical cyclone activity. J. Clim. 27 (21), 7994–8016. https://doi.org/10.1175/JCLI-D-14-00158.1.

Von Uexkull, N., Buhaug, H., 2021. Security implications of climate change: a decade of scientific progress. https://doi.org/10.1177/0022343320984210.

Von Uexkull, N., Croicu, M., Fjelde, H., Buhaug, H., 2016. Civil conflict sensitivity to growing-season drought. Proc. Natl. Acad. Sci. U. S. A 113 (44), 12391–12396. https://doi.org/10.1073/PNAS.1607542113/SUPPL_FILE/PNAS.201607542SI.PDF.

Waaben Thulstrup, A., Habimana, D., Joshi, I., Mumuli Oduori, S., 2020. Uncovering the challenges of domestic energy access in the context of weather and climate extremes in Somalia. Weather Clim. Extrem. 27, 100185. https://doi.org/10.1016/J.WACE.2018.09.002.

Wang, X., Jiang, D., Lang, X., 2020. Future changes in Aridity Index at two and four degrees of global warming above preindustrial levels. https://doi.org/10.1002/joc.6620.

WFP, 2021. SAVING LIVES CHANGING LIVES WFP's Work in Enabling Social Protection in Somalia Highlights of the World Food Programme's Contributions to Social Protection in a New Normal.

WFP, 2022a. Horn of Africa: extreme drought deepens hunger in a region facing conflict | Africa Renewal. https://www.un.org/africarenewal/magazine/november-2022/horn-africa-extreme-drought-deepens-hunger-region-facing-conflict.

WFP, 2022b. Kenya emergency | world food programme. https://www.wfp.org/emergencies/kenya-emergency.

WHO, 2023. From insight to action: examining mortality in Somalia HIGHLIGHTS. https://reliefweb.int/report/somalia/mortality-among-populations-southern-and-central-somalia-affected-severe-food.

WMO. (n.d.). Meteorological and humanitarian agencies sound alert on East Africa | World Meteorological Organization. Retrieved October 30, 2023, from https://public.wmo.int/en/media/news/meteorological-and-humanitarian-agencies-sound-alert-east-africa.

World Bank, 2013. Growing Africa. https://documents1.worldbank.org/curated/en/327811467990084951/pdf/756630v10REPLA0frica0pub03011013web.pdf.

World Bank, 2019. Impact of drought on poverty in Somalia. https://papers.ssrn.com/abstract=3313863.

World Bank, 2020. Somalia - Country Environmental Analysis : Diagnostic Study on Trends and Threats for Environmental and Natural Resources Challenges. World Bank Group.

World Bank, 2022. Developing a state-led social safety net system to boost human capital and build resilience in Somalia: the baxnaano program. https://www.worldbank.org/en/results/2022/10/10/developing-a-state-led-social-safety-net-system-to-boost-human-capital-and-build-resilience-in-somalia-the-baxnaano-prog.

Xu, C.Y., Singh, V.P., 2002. Cross comparison of empirical equations for calculating potential evapotranspiration with data from Switzerland. Water Resour. Manag. 16 (3), 197–219. https://doi.org/10.1023/A:1020282515975.

Yang, W., Hsieh, T.L., Vecchi, G.A., 2021. Hurricane annual cycle controlled by both seeds and genesis probability. Proc. Natl. Acad. Sci. U. S. A 118 (41), e2108397118. https://doi.org/10.1073/PNAS.2108397118/SUPPL_FILE/PNAS.2108397118.SAPP.PDF.

Yayeh Ayal, D., Yohannes Kebede, H., Belay, A., Mekuyie, M., 2022. Climate variability and indigenous adaptation strategies by Somali pastoralists in Ethiopia. https://doi.org/10.21203/rs.3.rs-1990099/v1.

Zachariah, M., Kumari, S., Mondal, A., Haustein, K., Otto, F.E.L., 2023. Attribution of the 2015 drought in Marathwada, India from a multivariate perspective. Weather Clim. Extrem. 39, 100546. https://doi.org/10.1016/J.WACE.2022.100546.

Zhang, D., Liu, X., Zhang, L., Zhang, Q., Gan, R., Li, X., 2020. Attribution of evapotranspiration changes in humid regions of China from 1982 to 2016. J. Geophys. Res. Atmos. 125 (13). https://doi.org/10.1029/2020JD032404.

Zhao, H., Ma, Y., 2021. Effects of various driving factors on potential evapotranspiration trends over the main grain-production area of China while accounting for vegetation dynamics. Agric. Water Manag. 250, 106854. https://doi.org/10.1016/J.AGWAT.2021.106854.

Zscheischler, J., Lehner, F., 2022. Attributing compound events to anthropogenic climate change. Bull. Am. Meteorol. Soc. 103 (3), E936–E953. https://doi.org/10.1175/BAMS-D-21-0116.1.